Application of Very High Resolution Imagery and Aerial Photography for Estimation of Above Ground Biomass/Carbon of Trees Outside Forest

SEMHAR KIFLAY ANDEMICHAEL

SUPERVISORS:
Ir. L.M. Van Leeuwen
Dr I.C. Van Duren

APPLICATION OF VERY HIGH RESOLUTION IMAGERYAND AERIAL PHOTOGRAPHY FOR ESTIMATION OF ABOVE GROUND BIOMASS/CARBON OF TREES OUTSIDE FOREST

SEMHAR KIFLAY ANDEMICHAEL
NRM15: S6025331
Enschede, The Netherlands, February, 2017

Thesis submitted to the Faculty of Geo-Information Science and Earth Observation of the University of Twente in partial fulfilment of the requirements for the degree of Master of Science in Geo-information Science and Earth Observation.
Specialization: Natural Resources Management

SUPERVISORS:
Ir. L.M. Van Leeuwen
Dr I.C. Van Duren

THESIS ASSESSMENT BOARD:
Dr. Y.A. Hussin (Chairman)
Dr. ir. Wietske Bijker (External Examiner, ITC-EOS)

APPLICATION OF VERY HIGH RESOLUTION AND AERIAL PHOTOGRAPHY FOR ESTIMATION OF ABOVE GROUND BIOMASS/CARBON OF TREES OUTSIDE FOREST

ABSTRACT

Trees which are found both inside and outside forest environments if managed significantly, they have an essential role in climate change mitigation and adaptation. Effective management of trees both inside and outside forests secures and maximizes the contribution of trees to climate change mitigation actions. Similar to trees inside forest environments, tree resources outside the forest (TOF) play a significant role in climate change mitigation actions by storing carbon and providing fuel to substitute fossil fuels. Hence quantitative and qualitative assessment of TOF AGB/carbon is vital to understand the contribution of TOF with regards to climate change mitigation actions. However the heterogeneity and complexity of TOF systems in terms of spatial distribution, low tree density and occurrence pattern pose a number of difficulties in evaluating accurately these tree resources.

In this study the potential of very high resolution satellite imagery and aerial photography for estimation of AGB/carbon was explored using the object based image analysis (OBIA) and Fourier textural ordination (FOTO) method. First AGB/carbon was calculated based on a previously established allometric equation using tree DBH measurements collected from field. The DBH measurement has shown a significant difference among the patch TOF configuration and linear TOF configuration with a p value<0.05. Hence AGB/carbon estimation based on field data was separately calculated for linear and patch TOF configuration. OBIA was then employed to segment crown projection area (CPA) of trees from the very high resolution Pleiades-1B imagery. The segmented CPA was then correlated with field measured DBH for different configuration of TOF to examine whether there is sound relationship with segmented CPA and field measured DBH. It was observed that trees in linear TOF configuration has a strong relationship with field measured DBH than trees on patch TOF configuration with R^2=0.78 and R^2=0.88 for patch and linear TOF configuration respectively. A non-linear regression model was fitted between the remotely sensed independent variable which is CPA and the dependent variable carbon to estimate carbon stock in the study area for linear and patch TOF configuration. The developed model was validated by plotting the predicted carbon against the observed carbon.

In addition to OBIA method the FOTO method was also used based on the aerial photography acquired from Google Earth platform. Three texture indices (TC) where selected as predictors of AGB/carbon of patch configuration TOF by using the 2D fast Fourier transform (2DFFT) algorithm in MatLab and principal component analysis. The relationship between FOTO texture indices and field derived AGB/carbon was calibrated using a linear multiple regression model. The developed model was then validated by using the field measure AGB/carbon of patch TOF configuration.

The OBIA method was found to be successful in predicting the AGB/carbon of both the linear and patch TOF configuration at R^2=0.86 and R^2=0.75 respectively. On the contrary the FOTO method was found suitable only for the prediction of AGB/carbon of patch TOF configuration. However the developed model for estimation of carbon based on the FOTO derived texture indices was able to explain 68% of the variations in observed carbon stock of only patch TOF configuration in the study area. Hence the study explored the merits of a freely available aerial photography from Google earth against very high resolution commercial satellite imagery for the estimation of AGB/carbon of the two main TOF configurations.

Key words: trees outside the forest, object based image analysis, Fourier textural ordination, above ground biomass

ACKNOWLEDGEMENTS

First and for most praise be to the Almighty GOD for safeguarding me and for being my source of everlasting inspiration and strength along the course of my MSc study.

I am sincerely grateful to the Joint Japan World Bank Graduate scholarship program (JJ/WBGS) for opening the door of endless opportunities to pursue my MSc study in the field of remote sensing and GIS for natural resource management.

I would like to extend my deepest appreciation and gratitude to my first supervisor Ir.L.M.Van Leeuwen, Whose relentless guidance, technical support and encouragement has made my MSc Research journey enthusiastic and unforgettable. Indeed this research wouldn't have been complete without her continuous assistance and motivation. Thank you.

I am also deeply in debt for my second supervisor Dr I.C. Van Duren for her constructive and positive feedback especially during the writing process of my MSc thesis. I am more than humbled to have you as my second supervisor. Thank you.

I would like to extend my sincere gratitude to Dr. Y.A. Hussin for the constructive comments he gave me during my proposal and mid-term presentation which was very helpful in shaping my MSc. Thesis.

My heartfelt appreciation also goes to the staff of faculty of Geo information Science and Earth observation (ITC) in general and the department of Natural Resources (ITC-NRS) in particular for their hospitable and very welcoming attitude.

To my fellow NRM and GEM classmates class of 2015-2017 thank you so much for the memorable time we had together. I wish you success in your future carrier path. I would like also to extend my heartfelt appreciation to my field work partner Mostarin Ara for the unforgettable time and fun we had together during the field work.

My kind gratefulness goes to my ITC alumni friends from my home country Eritrea; Mr. Semere Tesfai Abrham and Mebrat Tikabo Sium for their genuine support and encouragement.

My deepest thankfulness also goes too to my fellow countrymen; Ghebregziabher Yemane, Yonas welday and Ezra Weldengus for your sincere accompany and sweet memories.

Finally my deepest appreciation goes to my beloved family for their endless Love and support. To my mother and father for your prayers and inspiration. I am also grateful to my two little sisters for their words of encouragement and support. May God bless you all.

Semhar Kiflay Andemichael
Enschede, The Netherlands
February, 2017

Dedicated to My Family the Source of My Love & Inspiration……

Table of Contents

1. Introduction 11
   1.1. Background 11
   1.2. Problem Statement and justification 12
   1.3. Research Objectives 14
2. Literature review 16
   2.1. Definitions and concepts of trees outside the forest (TOF) 16
      2.1.1. Functions of TOF 16
      2.1.2. Classification of TOF 17
   2.2. Biomass and carbon 18
   2.3. Crown projection area (CPA) 19
   2.4. Allometric equation 19
   2.5. OBIA (object based image analysis) 19
      2.5.1. Multi-resolution segmentation 20
   2.6. FOTO (Fourier Textural Ordination) 21
3. Research Material and Method 22
   3.1. Study area 22
      3.1.1 Location and climate 22
      3.1.2 Criteria for the selection of study area 22
      3.1.3 TOF in the study area 22
   3.2. Materials 24
      3.2.1 Remote sensing dataset 24
      3.2.2 Field instrument 24
      3.2.3 Software and tools 25
      3.3. Research Methods 25
      3.3.1 Pan-sharpening of Pleiades-B1 image 26
      3.3.2 Visualization of TOF configurations in the study area 27
      3.3.3 Sampling Design 27
      3.3.4 Field data collection 27
      3.3.5 Image segmentation of Pleiades-1B satellite imagery 28
      3.3.6 FOTO method 32
      3.3.7 Above ground biomass (AGB) and carbon stock calculation based on field data 33
      3.3.8 Regression analysis and model validation 34
      3.3.9 AGB and Carbon Mapping 34
4. Result 35
   4.1. Descriptive analysis of field data 35
   4.2. Multi-resolution segmentation 38
   4.3. Segmentation validation 38
   4.4. AGB/carbon modelling based on OBIA 39
      4.4.1. Relationship between DBH and CPA of linear and patch TOF configuration 39

4.4.2.Model development 39
4.4.3.Model Validation 41
4.4.4 Carbon stock mapping of linear and patch TOF configuration 42
4.5 Modelling of AGB/carbon based on FOTO derived texture indices 47
4.5.1.Carbon stock mapping based FOTO 47
4.6 Comparison of FOTO and OBIA method in TOF AGB/carbon estimation 48
5. Discussion 50
5.1. Distribution of field measured data 50
5.2. Segmentation accuracy 50
5.3. FOTO method 51
5.4. AGB/Carbon estimation of TOF 53
5.4.1 Relationship of remotely sensed CPA and field measured DBH in patch and linear TOF configuration 53
5.4.2 Modelling of carbon from CPA 54
5.4.3 Modelling of carbon from texture indices 54
5.4.4 Comparison of FOTO estimated Carbon and OBIA estimated Carbon for patch TOF configuration 54
5.5. Sources of uncertainity in carbon modelling 55
6. Conclusion 58

LIST OF FIGURES

Figure 1. Land classification framework and the position of TOF (Foresta et al., 2013) 16
Figure 2. Illustration of crown projection area (CPA) and other tree dimensions 19
Figure 3. Illustration of multi-resolution image segmentation (Definiens, 2007) 20
Figure 4. AGB using FOTO analysis of Google earth imagery (Ploton et al., 2012) 21
Figure 5. Location map of Google earth image (bottom left) and Pleiades-1B (top right) of the study area 23
Figure 6. Flowchart of Research Methodology 26
Figure 7. Estimation of scale parameter using the (ESP) tool 28
Figure 8. Multi-resolution segmentation rule set (workflow) 29
Figure 9. a) Multi-resolution
b) Watershed process
c) Morphology process 30
Figure 10. a) Before Rel.to border algorithm
b) After Rel.to border algorithm 30
Figure 11. Topological relationship of segmented and manually digitized objects (Zhang, 1996) 31
Figure 12. Windowed aerial photography from Google Earth image 32
Figure 13. Pie- chart percentage of trees sampled for different TOF configurations 35
Figure 14. Boxplot of different TOF configurations DBH 36
Figure 15. Percentage of different tree species in different classes 37
Figure 16. Illustration of the final output of the multi-resolution segmentation process in eCognition 38
Figure 17. Comparison of segmented and manually digitized polygons 38
Figure 18. a) Scatter plot of CPA & DBH of linear configuration
b) Scatter plot of DBH & CPA of patch configuration 39
Figure 19. Scatter plot of carbon and CPA 40
Figure 20. Scatter plot of CPA and Carbon of trees on patches 41
Figure 21. Scatter plot of model validation for linear formation TOF configuration 42
Figure 22. Scatter plot of model validation for Patch TOF configuration 42
Figure 23. Carbon Stock Map of Linear Configuration of TOF of the Study Area 45
Figure 24. Carbon Stock Map of Patch Configuration of TOF of the Study Area 46
Figure 25. Scatter plot of FOTO carbon estimation validation 47
Figure 26. FOTO Derived Carbon Stock Map of Patch Configuration of the Study Area 48
Figure 27. Spectral signature of different land cover classes in the study area 51
Figure 28. Comparison of different window sizes against PCA scores (Proisy et al., 2007) 52
Figure 29. Example of windowing the aerial photography 53
Figure 30. the level of tree intermingling (Shimano, 1997) 53
Figure 31. Shadow of trees along a windbreak configuration 56

LIST OF TABLES

Table 1 Specifications of Pleiades-1B image 24
Table 2. Field data collected and instruments used 25
Table 3. List of software's used and corresponding functions 25
Table 4. Statistical summary of DBH measurement in the different TOF configuration 35
Table 5. Statistical summary of height measurements in different TOF configurations 36
Table 6. Normality test result of DBH and Height measurements 36
Table 7. Paired sample test of the three classes in linear configuration trees 37
Table 8. Paired sample t test among DBH of trees in patches and linear formation TOF 37
Table 9. Result of regression analysis of linear formation trees 40
Table 10. Summary of regression analysis for patches 41
Table 11. Pearson correlation test between field measured carbon and OBIA predicted carbon 49
Table 12. Pearson correlation test between field measured carbon and FOTO predicted carbon 49

LIST OF EQUATIONS

Equation 1: Over segmentation 31
Equation 2: Under segmentation 31
Equation 3: Measure of goodness 31
Equation 4: Window Size 32
Equation 5: AGB calculation 33
Equation 6: Carbon stock calculation 34
Equation 7: RMSE 34
Equation 8: Carbon stock calculation for linerar TOF configuration 40
Equation 9: Carbon stock calculation for patch TOF configuration 41

LIST OF APPENDICES

Appendix 1: Histogram of DBH for different configuration of TOF 63
Appendix 2: Histogram of Height for different TOF configurations 63
Appendix 3: Collinearity test between CPA and DBH of patch configuration TOF 64
Appendix 4: Collinearity test between CPA and DBH of linear configuration TOF 64
Appendix 5: Rule set for multi-resolution segmentation of Pleiades-1B satellite imagery 65
Appendix 6: Field data collection record sheet 66
Appendix 7: Photos from the field 67

1. INTRODUCTION

1.1. Background

Earth's climate is warming at an unprecedented rate. Burning of fossil fuels and consequent increase of carbon dioxide (CO_2) concentration in the atmosphere is identified as the prime cause for the rise in atmospheric temperature by 0.5°C in the past 100 years and it is predicted to rise from 0.6 to 5°C in the coming 100 years (IPCC, 2000). In the fight against global warming trees have a vital role to play being the largest terrestrial reservoirs of carbon after coal and oil (Baro et al., 2014). Trees act as a sink for CO_2 by fixing carbon during photosynthesis and storing carbon as biomass. This is a major pathway during which carbon is removed from the atmosphere making forest ecosystems primary focus in climate change discussions. In addition to forest ecosystems, tree resources outside the forest also have great potential for atmospheric carbon sequestration (Singh & Chand, 2013). Hence the current demanding issue of global warming presents "trees outside the forest" (hereafter referred as TOF) an opportunity to serve as potential carbon sinks and thus perhaps be could incorporated in the future carbon trade negotiations (Stoffberg et al., 2010).

The world has billions of trees that are not included in the class of forest nor integrated with the category of other wood land. Presence of favourable ecological conditions in any given landscape might induce tree growth in different quantity and spatial arrangements (Foresta et al., 2013). Different countries have various valid ways of defining what a forest is and what a woodland is according to their list of predefined standards, however regardless of how a forest or a woodland is defined all trees can never be contained within that definition (Foresta et al., 2013). To this Food and Agriculture Organization (FAO) tailored a definition in an endeavour to clearly distinguish tree resources which are absent from the class of forest and woodlands. According to FAO by default TOF are tree resources which don't belong to the category of forest areas and other woodland (FAO, 2003). Hence TOF exhibit a wide spectrum ranging from single standalone trees on homesteads to groups of trees in patches that don't qualify to be forest.

TOF grow in the form of three main patterns or configurations, namely compact tree patches, scattered standalone trees and trees in linear formations (FAO, 2003). Patches are group of trees that constitute an area less than 0.5 hectare (Ha) of land where as linear TOF configuration are trees planted in the form of continuous lines such as roadside trees and windbreaks covering an area with length more than 25 meter (m) and width less than 20 meters. As for scattered standalone trees there is no specific area threshold however in order for a tree to be considered as a single standalone tree the stem to stem distance with a neighbouring tree if there is any, should be more than 10m while the crown to crown distance should be more than 7.5 m (Singh, 2013; Foresta et al., 2013).

The above mentioned TOF configurations can be found manifested in different land cover land use classes such as in agricultural lands in the form of windbreaks, on built up areas in the form of road side plantations, in barren land in the form of single standalone trees and in the form of orchards or agro-forestry plantations. In terms of spatial arrangements they may be found scattered on farmlands or growing continuously along roads, canals and water courses or in small aggregates such as blocks of trees (Alexandrov et al., 1999).

The need for reporting carbon stocks in a detailed and systematic way that embraces all trees which are inside and outside a forest have prompted the demands for accurate surveying methods (IPCC, 2007). Current assessment of TOF carbon sequestration ability heavily relay on field measured tree variables such as diameter at breast height, tree height or other easily measurable tree allometry that can be related to standing biomass (dry mass) using certain allometric equations and consequently converted to carbon stock (Stoffberg et al., 2010). However biomass/carbon assessment of TOF based on traditional field surveys solely is less effective because it is time consuming, date lagged and often too expensive given the low density and wide distribution of TOF elements (Xie et al., 2008). On the other hand remote-sensing data obtained through instruments mounted on satellites or airplanes can be processed to give estimation of tree biomass that can easily be converted using statistical relationships to carbon measurements (Gibbs et al., 2007). According to the IPCC (2004) report, remote sensing is becoming the most suitable and cost effective technique applied for quantification of above ground biomass (AGB) facilitating extensive estimation of carbon stocks.

Remote sensing data can provide comprehensive and reliable information on TOF presence, spatial distribution, type, quality, and temporal changes which covers larger areas (Foresta et al., 2013). These data can be acquired through various remote sensing techniques, such as optical remote sensing, Radar, Light Detection and Ranging (LiDAR) and aerial photography (Xie et al., 2008). Previous studies in TOF have used different remote sensing data from satellite imagery in combination with field collected data to assess TOF (Kleinn, 2000). Aerial photography from Google Earth (hereafter referred as GE) however is so often used only for the purpose of visualization, sampling and classification of different TOF categories.

1.2. Problem Statement and justification

International institutions such as United Nation Framework Convention on Climate Change (UNFCCC) require incorporation of carbon information for trees both inside and outside forest to cater holistic decision with regards to climate change mitigation engagements (Schnell, 2015; IPCC, 2007; Foresta et al., 2013). However in proportion to the number of studies conducted to quantify the significant role of trees inside forests in absorbing, storing, and releasing carbon little has been done for the very same roles of trees that exist outside the forest (Kleinn, 2000). But the need to bridge the knowledge gab about trees that exist inside and outside the forest all together has been gaining attention recently due to the growing awareness of climate change issues and its mitigation measures with the appreciation of the role of trees inside and outside forests for carbon sequestration (Foresta et al., 2013).

Reliable data on the extent, location, distribution and biophysical information of TOF both on global and national scale is always difficult to find (Zomer et al., 2014). The most frequently mentioned reason for insufficient information about TOF is that assessing TOF poses a number of challenges as compared to assessing forests (Schnell, 2015; Johnson et al., 2015). TOF doesn't constitute a land category rather it is a resource that occurs in various non-forest land cover land use classes. Moreover the complexity and heterogeneity of TOF systems and their limited spatial footprint is among the various setbacks that hinder efficient assessment of TOF (Zomer et al., 2014). Thus even though TOF have the ability to influence and affect climate change they are often neglected because their ecosystem services in relation to this issue is not well quantified (Nowak et al., 2013). Therefore prior to assessing the role of TOF in carbon sequestration by measuring AGB, a robust and consistent method for classification and mapping of the different TOF configurations should be considered (Long & Nair, 1999).

Quantification of carbon stock and flux of trees depend on the estimation of the living AGB which is the largest carbon pool with in each individual tree (Gibbs et al., 2007). Currently AGB estimation of TOF is most often done by using established forest allometric equations that rely on field measured tree variables

(Foresta et al., 2013). However traditional ground based data is acquired at an expensive cost, covers small area and its labour intensive. In contrary current advances in the remote sensing science provides a number of alternative ways of assessing tree biophysical parameters such as AGB efficiently and less costly (Schnell et al., 2015). But the difference in spatial and spectral resolution of various sensors influences the accuracy of assessing the AGB/carbon of TOF (FAO, 2003). Therefore the sparse tree density and the heterogonous landscape TOF exist require a correct choice of remote-sensing imagery and processing method to be used.

Apart from being expensive very high resolution (hereafter referred as VHR)remote sensing images are currently identified to be potential solutions to assess the ABG/carbon of trees (Hussin et al., 2014). In the case of TOF high resolution images were utilized so far as supplementary data mostly for the purpose of classification, mapping and visualization of different categories of tree resources outside the forest (Pujar et al., 2014; Meneguzzo et al., 2013; Singh & Chand, 2013; Schnell et al., 2015). In their evaluation of the most suitable spatial resolution of a remote sensing data for assessing TOF, Schnell et al. (2015), outlined that VHR imagery can be promising technique when complemented with object based image classification (OBIA) not only for mapping of TOF but for estimation of TOF biophysical parameters such as AGB. OBIA divides a given remote sensing imagery into a number of image objects similar to the way human beings conceptualize those objects in real life (Hay & Castilla, 2006). However OBIA aided AGB/carbon assessments are most often done for tree resources which are found on forest environments (Zomer et al., 2014). Nevertheless the contextual and spectral attributes present in OBIA can be efficient to single out TOF tree crowns from the complex and very heterogeneous landscape where TOF are present for AGB/carbon assessment of TOF.

Aerial photography available in GE is free and it supports wall-to-wall assessment of TOF. Unlike trees inside forest environments TOF have a relatively low tree density per any given area and wider distribution. Therefore the freely accessible images in the GE interface allow TOF assessment in any preferred scale. However Aerial photography has a low spectral resolution when compared to satellite imagery of the same spatial resolution. Hence the relatively poor spectral resolution of aerial photography makes pixel and object based image analysis for AGB/carbon estimation very difficult (Hu et al., 2013). Thus with regards to TOF the use of aerial photography is most often used to visual image interpretation and sampling TOF elements (Kleinn, 2000). The richness in texture and high spatial resolution of aerial photography compensates for the low spectral resolution of this data and thereby enabling a number of textural operations such as Fourier textural ordination (FOTO). The FOTO method depends on textural indices (TC) to estimate biomass (Couteron et al., 2005). The method employs the 2DFFT algorithm in MatLab to convert the spatial domain of an image in to a frequency domain. The obtained frequency domain is further processed to produce TC which are used as predictors of AGB (Bastin, 2014).

Hence this study aims to explore and compare the estimation of AGB/carbon of TOF from VHR satellite imagery using the OBIA and aerial photography from GE using the FOTO method in the study area which is located in Gronau Germany.

1.3. Research Objectives

- The main objective of this research is to compare above ground biomass and carbon estimation of trees outside the forest in the study area using Object based image analysis (OBIA) and Fourier textural ordination (FOTO) method based on very high resolution satellite imagery and an aerial photography from Google earth.

Specific Objectives

- To assess the segmentation accuracy of Object based image analysis (OBIA) in delineating tree crowns of different trees outside the forest (TOF)configurations
- To assess the relationship between tree DBH measured from field and CPA segmented from very high resolution satellite imagery of different trees outside the forest (TOF) configurations
- To assess the relationship between above ground biomass (AGB) derived from Fourier textural ordination (FOTO) method and above ground biomass (AGB) derived from field data of trees outside the forest (TOF).
- To develop a model for assessing above ground biomass (AGB) and carbon of trees outside the forest (TOF) from very high resolution satellite imagery and aerial photography from GE of the study area.

Research questions

- How accurately can tree crowns in different trees outside the forest (TOF) configurations be segmented?
- How significant is the relationship of segmented CPA and field measured DBH of trees between different trees outside the forest (TOF) configurations?
- How significant is the relationship between FOTO predicted above ground biomass (AGB)/carbon and field calculated above ground biomass (AGB)/carbon of trees outside the forest (TOF)?
- Which of one of the two remote sensing images used is more accurate for estimation of above ground biomass/carbon of trees outside the forest when compared with field measured above ground biomass/carbon?

Hypothesis

1. H0: The segmentation accuracy for TOF tree crown segmentation of the different configurations using VHR imagery is < 70%.

   Ha: The segmentation accuracy for TOF tree crown segmentation of the different configurations using VHR imagery is > 70%.
2. H0: There is no significant relationship between CPA from VHR imagery and DBH measured from the field in different TOF configurations at 95% confidence level

   Ha: There is significant relationship of CPA from VHR imagery and DBH measured from field between different TOF configurations at 95% confidence level

3. H0: there is no significant relationship between FOTO predicted AGB/carbon using aerial photography from Google earth and AGB/carbon measured from the field at 95% degree of confidence

   Ha: there is significant relationship between FOTO predicted AGB/carbon using aerial photography from Google earth and AGB/carbon measured from the field at 95% degree of confidence
4. H0: There is no significant relationship between FOTO predicted and OBIA predicted AGB/Carbon estimation with field measured AGB/carbon

   Ha: There is significant relationship between FOTO predicted and OBIA predicted AGB/Carbon estimation with field measured AGB/carbon

2. LITERATURE REVIEW

2.1. Definitions and concepts of trees outside the forest (TOF)

Forest and TOF are two features of the same resource hence the definition given to tree resources inside and outside the forest varies greatly from country to country however they all have certain similarities (Kleinn, 2000). TOF are trees that do not comply with the criteria of Forest, so the TOF realm depends on the definition used for Forest. Hence any tree resource that is not considered as a forest in any specific country is classified as tree resources that exist outside a forest ecosystem (refer to figure 1) (Foresta et al., 2013). The whole idea of viewing trees outside the forest apart from the category of forests and other wood land emerged in 1995 (Foresta et al., 2013). The term was introduced with the intention of emphasizing the importance of TOF for ensuring sustainable livelihood on one hand and raising awareness with regards to TOF for landscape restoration on the other hand.

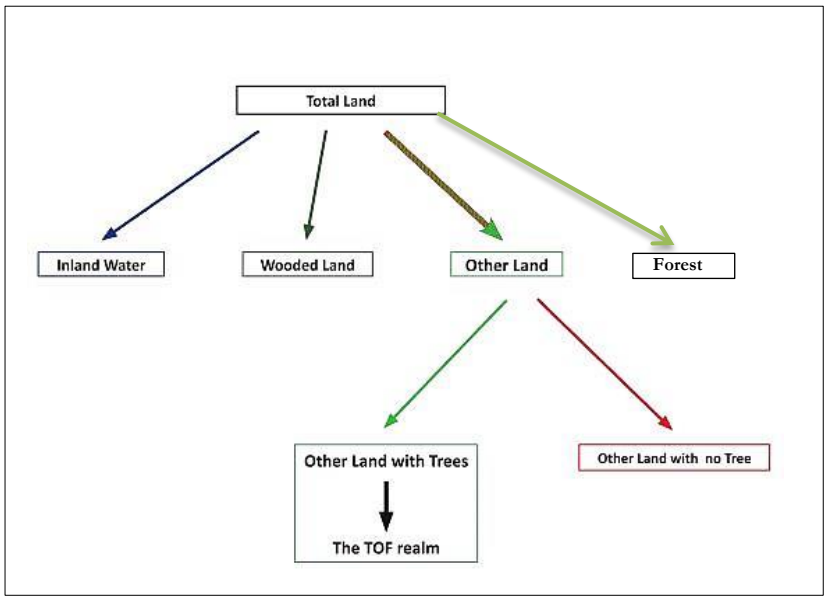

Figure 1. Land classification framework and the position of TOF (Foresta et al., 2013)

2.1.1. Functions of TOF

The number of ecological, economic and social functions offered by TOF range from recreational services to environmental functions such as carbon sequestration (Davies et al., 2011). TOF influence local climate and carbon cycles and contribute their share to mitigate climate change through carbon sequestration (David et al., 2012). For instance trees outside the forest constitute 516 Terra gram of carbon in China with annual carbon sequestration rate of 19.1 terra grams (Guo et al., 2014). Similarly in USA and India TOF store 700 and 931 terra gram of carbon respectively that means tree resources outside the forest make up 14% of the total carbon sequestered by US forests (Nowak et al., 2013; McPherson et al., 2013). Therefore various international organizations related to climate change mitigation activities such as the UNFCCC are interested on accurate information of TOF as it relates to international reporting obligations.

Moreover TOF also provide a wide range of services related to other socio-economic services which are provided by forests such as timber and fodder (Pujar et al., 2014). Most of the time forest areas are found

in the form of forest reserves or national parks and they are inaccessible because of restrictions and national laws employed on how and when to use forest trees (Foresta et al., 2013). Therefore TOF can fill the service gap and in some places if they are present in enormous amount they can even substitute the services rendered by forests.

According to the reports of FAO and Forest Resource Assessment (FAO, 2003), TOF play a vital role on promoting sustainable livelihoods by enhancing the contribution of TOF through sustainable and integrated land management. TOF provide a variety of goods and services, some of which are independent of land use while others are land-use specific (Foresta et al., 2013). Agroforestry and shifting cultivation are some of the agricultural practices that enhance tree regeneration while at the same time taking advantage of the land for agricultural purposes. Moreover TOF render variety of goods and services that can positively impact income level of people especially in rural areas by selling several of the goods and services that can easily be harnessed from TOF such as fruits, fuel wood and medicine (Foresta et al., 2013).

Tree resources which are not considered part of a forest also provide a wide range of services in urban areas which have trees inside and outside their peripheries (Nowak et al., 2013). Most cities are gifted with facets of trees in the form of recreational parks which are considered as TOF, these trees provide environmental and aesthetic function. Furthermore trees in urban areas also monitor local climate and contribute to air purification caused through anthropogenic pollution through their unique process of evapotranspiration and photosynthesis (Foresta et al., 2013).

2.1.2. **Classification of TOF**

Classification of TOF in a comprehensive manner is necessary to avoid the confusion and ambiguity related with this natural resource (Kleinn, 2000). An effective classification scheme is very useful for achieving reasonable uniformity between the objects of the inventoried resource and it encourages and simplifies the comparison of different research outputs of the same resource. Concerning TOF a clear classification scheme further enables easy representation and mapping of all the diversity embraced with in the TOF realm (Fernandez, 2003). However a common and conventional classification scheme with regards to TOF is often hard to find as there are several equally important criteria's were TOF can be grouped in to meaningful classes (Schnell, 2015). Both land cover and land use where TOF exist should be taken into consideration to avoid confusion and error in classification of TOF. For example a rubber plantations or trees in an agroforestry ecosystem would qualify as a forest if a classifications scheme is solely based on the percentage of land covered by tree crowns. Hence it is necessary to mutually consider the land cover and land use type where TOF exist for a clear and inclusive TOF classification (Kleinn, 2000).

Tree resources that exist outside the forest can be classified in to various classes according to various criteria. According to land use TOF can be classified as agroforestry, trees that grow during shifted cultivation, urban trees such as roadside trees and so on. TOF can also be classified in to different groups according to the function they serve. Windbreaks, fences and trees for scenic beauty are some of the TOF classes related to certain kind of function. However the most frequently adopted classification is based on the geometrical pattern TOF grow in certain landscape. This is the highly appreciated type of classification of TOF because it addresses and further more resolves the ambiguities that surround the classification of TOF to a certain reasonable level. According to Kleinn (2000) spatial arrangement or geometry of TOF

one of the two most practical principal attributes for designing an effective TOF classification system. Moreover geometry based classifications enables easy representation and mapping of TOF in a clear and homogenous manner (Fernandez, 2003). According to their geometrical configurations TOF are classified as:

1) Patch or blocks of trees: are group of trees which are doomed to be considered as non- forests because of the area they span (Forest et al., 2013). According to FAO (2003) all patches of trees which are found in a predominantly agricultural or urban land belong to tree resources outside the forest (see figure 5 page 23). In addition to that the term "tree" in TOF includes other resources as shrubs and palms in which some countries consider them as very important part of their resources (Schnell, 2015).

2) Linear formation trees: are tree lines: Linear tree formations include shelterbelts, windbreaks, living fences, hedges, tree lines, road trees etc. Most of the time they are closely linked to certain type of land use and, they are planted to supplement or serve a certain kind of land use system. In the study area the most reoccurring linear formation TOF are road side trees and boundary trees such as windbreaks.
Therefore the linear formation TOF are further divided in to three classes for the purpose of sampling and data analysis, namely windbreaks, single tree lines along roads and double tree lines along roads

a) **Windbreaks:** Windbreaks are plantation of trees in the form of a row to provide shelter from wind and soil erosion to the adjacent agricultural fields (Current, 2011). Most often a mixture of deciduous and coniferous plants is chosen for an effective and long lasting service (Weiderman, 2012), see figure 5 page 23.

b) **Single & double tree lines along the roads:** which are sometimes also called " tree avenue" are plantation of trees along small or big roads for the purpose reducing traffic speeds and to create safer walking environments for pedestrians in addition to their aesthetic services (Burden, 2006), see figure 5 page 23.

3) Standalone/individual trees: are trees which are found scattered in different land-cover/land-use classes serving different kind of purposes.

2.2. Biomass and carbon

Biomass is the total living or dead organic material of any plant which is found below or above ground per unit of an area occupied by the plant (IPCC, 2003). Biomass of a plant is further divided in to below and above ground biomass. Above ground biomass (AGB) refers to the organic material of a plant that is found above the soil whilst below ground biomass all the plant organic material that is found below the soil which is the plant root (Kajimoto et al., 1999). Carbon constitutes 45-50% of an oven dried biomass (Gibbs et al., 2007). Plants consume carbon dioxide from the atmosphere for the process of photosynthesis this is one of main routs carbon is removed from the atmosphere (IPCC, 2003). In an equilibrium state the rate of carbon removed from the atmosphere equals the rate carbon is released to the atmosphere. However nowadays the natural balance of carbon cycle is disturbed mainly due to several man made or anthropogenic activities (Poorter et al., 2011). The amount of carbon present with in the biomass of a given tree can be quantified in a number of ways. Among them is an allometric equation based biomass estimation. Allometric equations relate easily measurable tree dimensions such as diameter at breast height (DBH) and height to estimate biophysical parameters such as biomass (Gibbs et al., 2007). Biomass and carbon estimation also is possible based on a remotely sensed data given that it is validated with a field estimation (Gibbs et al., 2007).

2.3. Crown projection area (CPA)

Canopy projection area or canopy cover refers to the percentage of an area in the forest floor which is covered by the vertical projection of a tree crown (Jennings et al., 1999). CPA is one of the most important and commonly utilized tree variables for the estimation of biophysical parameters such as biomass especially from a remotely sensed data (see figure 2).

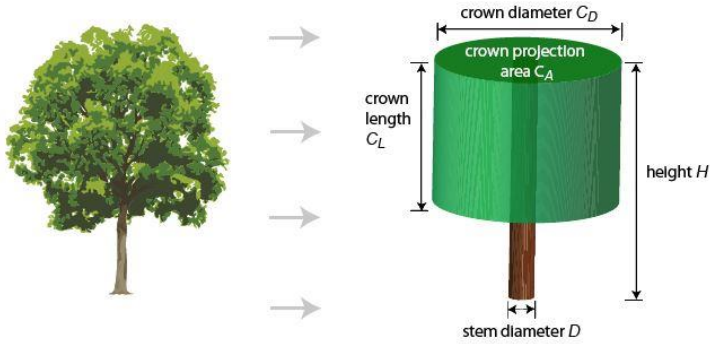

Figure 2. Illustration of crown projection area (CPA) and other tree dimensions
Source: (http://formind.org/model/what-are-the-main-processes-of-formind/growth/)

2.4. Allometric equation

Allometric equations are established equations which are formulated to assess properties of trees which are difficult to physically evaluate such as AGB/carbon based on other tree properties or dimensions which are fairly easy to measure. Tree DBH is one of the most commonly used biometric measurement which is used for formulation of allometric equations using empirical allometric models (Chave et al., 2014). Though there are also a number of allometric equations which utilize height measurement in combination with DBH measurements or only height measurements, the inclusion of tree height dimension has always been controversial (McHale etal., 2009). Tree height has often been ignored in carbon-accounting programs because measuring tree height accurately is difficult in forests especially in closed-canopy forests (Hunter etal., 2013).

2.5. OBIA (object based image analysis)

OBIA is an automated object based high resolution satellite imagery analysis which used to extract information from satellite images. Pixel-based classification methods fall short to satisfy classification accuracy acquired from very high-resolution images due to the fact that VHR images provide very abundant information (Burnett & Blaschke, 2003; Wei et al., 2005). This gave rise the need to develop a method which overcomes this limitations. In addition to the classification criteria's pixel based classifiers take in to consideration OBIA includes contextual information of objects to interpret an image into meaningful objects and their mutual relationships besides to single pixels. With respect to TOF the OBIA approach has produced satisfactory results in classifying and mapping different elements of TOF (Meneguzzo et al., 2013). OBIA starts by segmenting the image in polygons which are known as primitive image objects. Image segmentation is the process of partitioning an image into multi-pixel regions or image objects based on spatial, spectral and textural characteristics of pixels (Ryherd & Woodcock, 1996).

Successful image segmentation is the first and most important prerequisite for efficient OBIA because it is at this step that image objects are created through the aggregation of homogenous pixels. Segmentation process if done properly reduces the spectral variation of pixels with in the same class thereby contributing to highest classification and statistical accuracy (Dragut et al., 2010).

Traditional segmentation approaches are divided in to top-down and bottom-up segmentation approaches. The bottom up approach or commonly the region based approach entails the chessboard, quad tree based and multi-resolution segmentation whereas the top-down segmentation algorithm involves multi-threshold segmentation and spectral difference segmentation (Ouyang, 2015).

The bottom-up segmentation approaches starts with segmenting the image in to small regions and then categorize regions that correspond to a single object. On the other hand the top-down approach starts with larger objects and divides it in to smaller image objects. With regards to TOF multi resolution segmentation which is a bottom-up segmentation approach gives a satisfactory result in distinguishing and delineating TOF elements from the other non-TOF land cover classes and further mapping the three main TOF configurations (Herrera et al., 2004) .

2.5.1. **Multi-resolution segmentation**

Multi-resolution segmentation is an optimization procedure which minimizes the average heterogeneity and maximizes the respective homogeneity of pixels within image objects. In multi-resolution each pixel is assumed as a single object afterwards, groups of image objects (pixels) are merged to form object primitives, refer to figure 3 (Darwish et al., 2003). The merging process in the multi-resolution segmentation depends on the so called "local homogeneity criterion" that describes the similarity and dissimilarity between neighboring image objects. The homogeneity criterion consists of color (spectral values) and shape properties that is explained in terms of smoothness and compactness of image objects and it measures how homogenous or heterogeneous an image object is with neighboring objects (Ryherd & Woodcock, 1996). Based on the homogeneity criterion threshold set by the user the merging process in the multi-resolution segmentation clutch's image objects that fall within the defined threshold in to one group to create object primitives. The process ends when the smallest increase in the parameters of the homogeneity criterion surpasses the user defined Scale Parameter threshold.

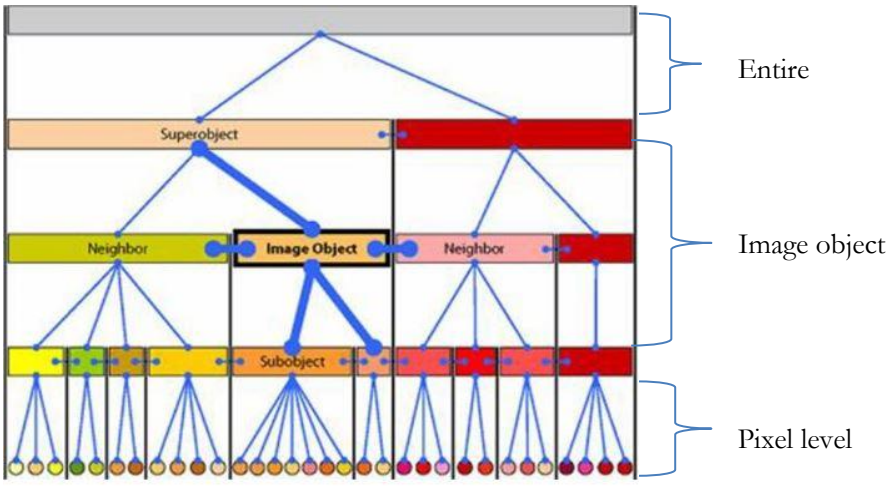

Figure 3. Illustration of multi-resolution image segmentation (Definiens, 2007)

2.6. FOTO (Fourier Textural Ordination)

Texture is defined as the spatial arrangement of achromatic or grey scale pixels in an image providing a measure of tonal change (Zhu, 1996). The Fourier textural ordination (FOTO) is a common method used for delineating surface structures explained in an array of tones ranging from white to black. Therefore to derive the quantitative textural measurements of such canopy grain one has to measure the degree of repetitiveness expressed in grey scale tones in frequency cycles/km(Proisy et al., 2011). This variation is measured by partitioning the image into equal size windows. This texture information can be extracted using 2 dimensional fast Fourier transform (2DFFT) techniques available in MatLab based on any remote sensing imagery but preferably high resolution imagery. The textural analysis using the 2DFFT method depends on the spatial distribution of continuous canopy grain of trees within a given scene and the shapes and size of their crowns. The 2DFFT algorithm in Mat-lab shifts canopy grain properties from the spatial domain to the frequency domain to generate texture indices which are used for the prediction of AGB/carbon. Ploton et al. (2012) discovered canopy texture has high correlation (70%) with AGB.

A recent advance in remote sensing data from aerial photography has added a new eye in the sky by providing extensive spatial coverage in a global scale such as GE imagery. Virtual interfaces such as GE nowadays provide bird's eye view of the earth's surface. GE releases free high spatial resolution images that are potentially instrumental for land use land cover mapping through remote sensing and GIS techniques. These data are of slightly lower quality when compared to the multispectral high resolution commercial images however they have proven to be efficient in deriving consistent characterizations of forest canopy crowns through textural analysis such as FOTO method (see figure 4) for AGB/carbon estimations (Barbier et al., 2012; Proisy et al., 2007; Ploton et al., 2012). Hence apart from LULC mapping some studies have managed to produce reliable biomass/carbon map based on aerial photography from GE for a tropical forest (Ploton et al., 2012).

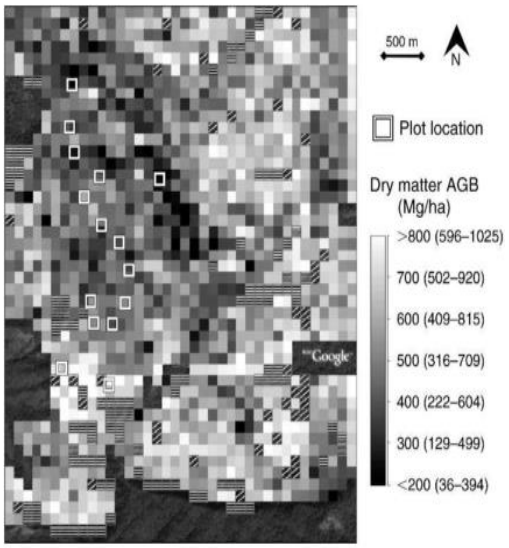

Figure 4. AGB using FOTO analysis of Google earth imagery (Ploton et al., 2012)

3. RESEARCH MATERIAL AND METHOD

3.1. Study area

3.1.1 Location and climate

The study area is located in North western part of Gronau Germany which is 10 kms east of Enschede, the Netherlands. It spans over an area of 40 km^2 both in north eastern part of Enschede and north western part of Gronau with an altitude of 81 meters ASL (above sea level) and with average temperature of 26^0c.

3.1.2 Criteria for the selection of study area

- Presence of all TOF configurations
- Accessibility and proximity

In addition to the above mentioned points it was important for the study area to fall in one image scene available in the GE platform.

3.1.3 TOF in the study area

The area is dominated by plain agricultural fields. It is also characterized by different TOF configurations scattered in the landscape (see figure 5). The study area contains all the three classifications of TOF based on geometrical configuration. The most dominant classification of TOF is linear configuration trees found in the form of windbreaks and single tree lines along the roads. Windbreak trees often exist related to individual agricultural fields serving as a border between two consecutive agricultural fields. Therefore almost all the agricultural fields in the study area possess some form of windbreak trees.

The second most dominant class of TOF in the study area is small forest patches that are considered as tree resources outside the forest. The trees with in this forest patches share higher resemblance with the temperate forest type which is persistent and indigenous to that place with mixed tree species such as scots pine, beech, spruce and other deciduous trees such as oak.

Standalone individual trees which are the third classification of TOF based on geometrical configuration are found in a very sparse and scattered manner in the study area. Moreover this class of TOF are most frequently located within private property of residents in the study area therefore this situation has made their accessibility for sampling very difficult. Hence in this research only the patches and all kinds of linear formation trees will be assessed for their AGB/carbon contribution in the study area.

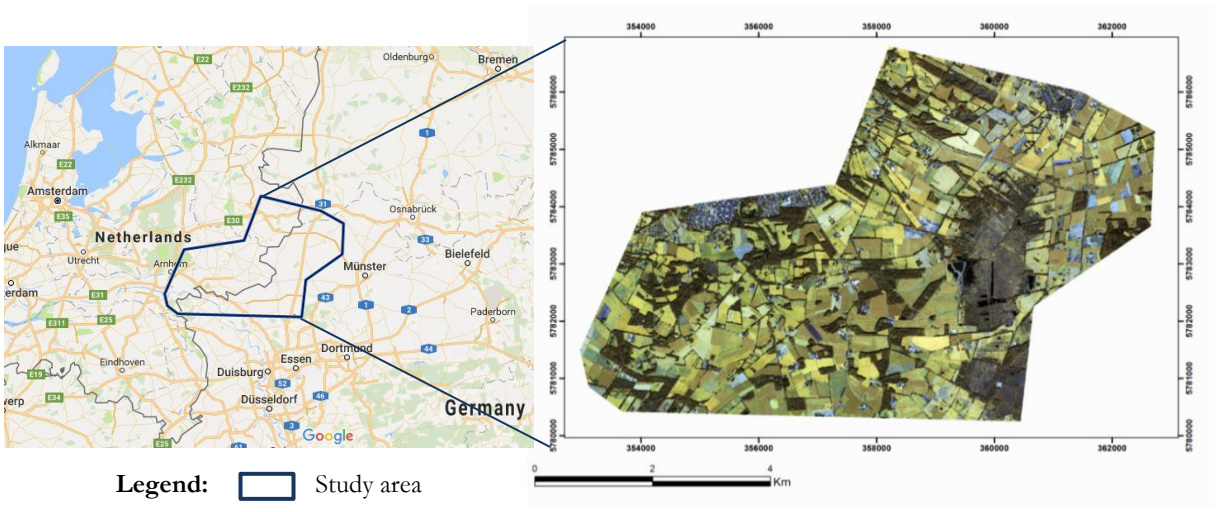

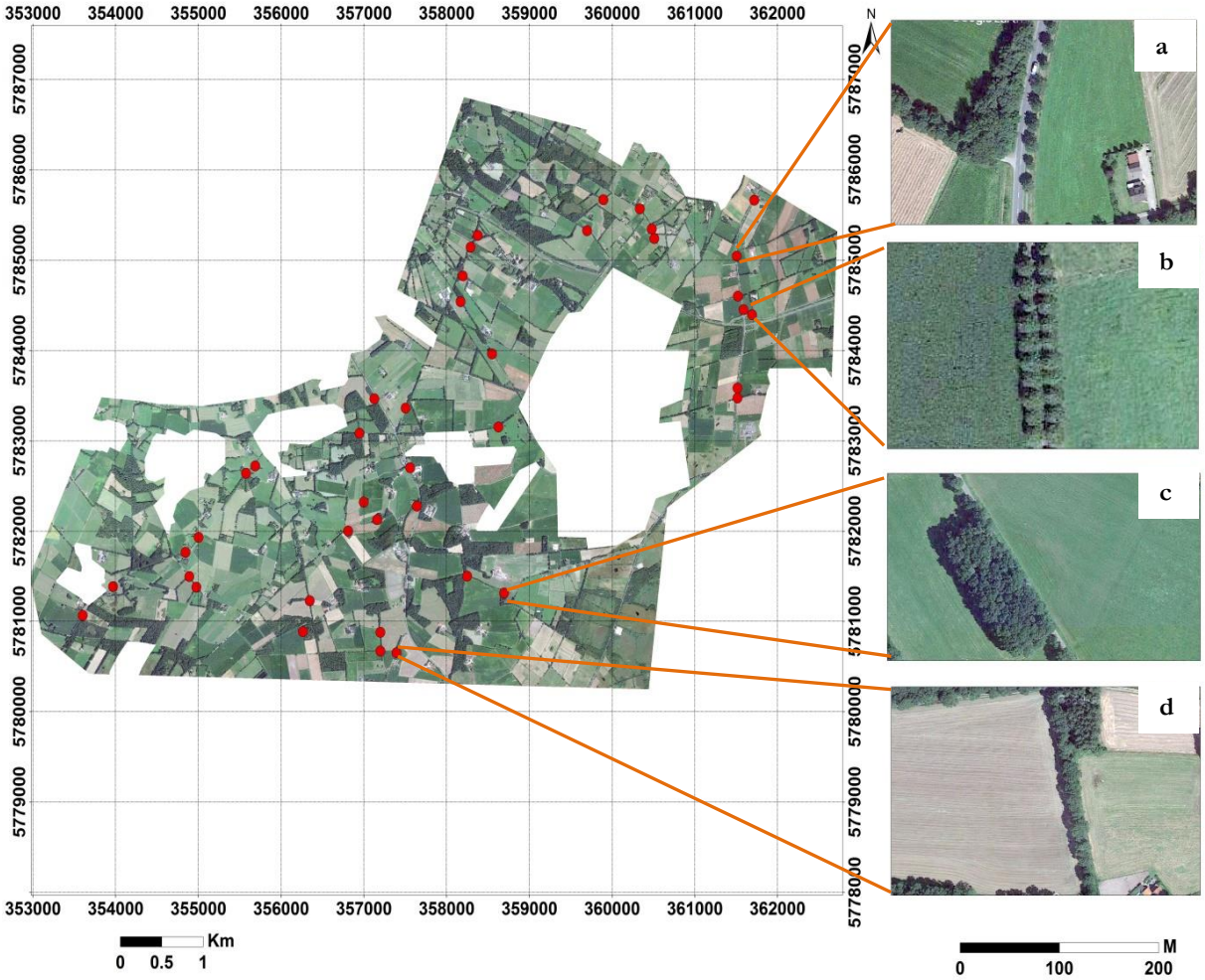

Figure 5. Location map of Google earth image (bottom left) and Pleiades-1B (top right) of the study area (a. Single line, b. Double line, c. Patch and d. Wind break)

3.2. Materials

3.2.1 Remote sensing dataset

a) **Pleiades-1B:** The Pleiades image comprises 4 bands of which there are in the visible electromagnetic spectrum namely, Blue, Green, Red and NIR_1. The image for the study area which includes both the multispectral and panchromatic is attained from the second generation Pleiades-1B sensor acquired on September 9 2015. It is an orthorectified image which is projected to a WGS 84 coordinate system. Further specification of the Pleiades high resolution image is in the table below.

Table 1 Specifications of Pleiades-1B image

Image specification	**Pleiades-1B**
Spatial resolution	0.5m panchromatic and 2m multispectral
Multispectral band wavelength	480-830nm
Acquisition data	2014 September 4th 10:50:42
Sun elevation (degree)	15^0
Off nadir	20km at nadir
Revisit time	daily
Coordinate system	WGS 1984
Cloud cover	1%

b) **Aerial photograph from GE:** The aerial photograph from GE was downloaded and the digitized boundary in kml format was opened in Google earth. Open source software called ElshayalSmart (Elshayal, 2015) was downloaded and used to extract the Google earth images that fall within the study area boundary. The advantage of Elshayal smart software is that it downloads orthorectified images along with the coordinate information from Google earth and hence the downloaded images can be directly utilized for any kind of GIS analysis without the need for georeferencing. A total of 705 strips of images acquired on July 20 2016 which covers the entire study area were downloaded. A scale (zoom level) of 80 m was used for downloading the images on Elshayal software to acquire a reasonably high spatial resolution of the Google earth imagery. It's evident that the zoom level in GE affects the spatial resolution of the downloaded image, hence for this study the zoom level was chosen based on the visibility of tree crowns. With this zoom level individual tree crowns were visible and this is important for the FOTO analysis on the downloaded aerial photography from GE. The individual images were then mosaicked to form one single image and converted from geographic coordinate system (latitude/longitude) to projected coordinate system (northing/easting) using Universal Transverse Mercator (UTM) projection in Arc GIS 10.

3.2.2 Field instrument

The field instruments for field data collection and measurement of tree parameters include: iPAQ, Garmin eTrex vista GPS, Laser range finder, densitometer, Suunto compass, Suunto Clinometer, Haga altimeter, caliper, diameter tape (5m), measuring tape (30m) and data record sheet to record tree parameter measurements were used. A detailed description of field instruments and their respective functions can be observed in table 3.

Table 2. Field data collected and instruments used

S/N	Tree Variable	Description	Instrument
1	Plot Coordinate	X & Y data of plot center	Garmin 12 XLS GPS receiver
2	Tree diameter at breast height (DBH)	Tree DBH>10cm	Diameter tape
3	Tree height	Height of the tree	Haga altimeter
4	Tree specie	Specie of each tree	
5	Canopy cover	Open/close canopy of sample plots	Ocular measurment
6	Configuration type/class	Geometrical configuration of each plot (patch, standalone tree or linear formation trees)	Ocular measurement
7	Road width	Width of the road for road side trees	Diameter tape

3.2.3 Software and tools

The research has utilized a number of software's starting from ElshayalSmart (Elshayal, 2015) for downloading rectified Google earth images until e-cognition and Matlab for running FOTO method data processing. eCognition software was used to make object based image classification to segment crown projection area (CPA) of trees from Pleiades-1B very high resolution imagery. ERDAS imagine 2013 was used for visualization, mosaicking of aerial photography from GE and ArcGIS 10.3 is used for further data analysis and processing of the outputs of the two images. MatLab software was used for texture analysis of GE imagery. Statistical analysis was done in R studio, SPSS and Microsoft Excel. Other Microsoft office 2010 like MS Word, MS Visio and MS PowerPoint were used for thesis write up and analysis. Below is a list of the software's employed in this research and their respective purposes.

Table 3. List of software's used and corresponding functions

Software	Purpose
ENVI 5.3	Pan sharpening of Pleiades-1B image
ElshayalSmart (Elshayal, 2015)	Downloading Google Earth image
eCognition developer 9.0.2	Image-segmentation and processing
ArcMap 10.3.1	Image processing and visualization
ERDAS IMAGINE 2015	Mosaicking of Google earth image and image processing
MatLab R2015b	2D Fourier transform textural analysis for Google earth image
R Studio, SPSS statistics22 and MS Excel	Statistical analysis and data presentation
Microsoft word 2010, Microsoft power point 2010 writing	Thesis writing and presentation

3.3. Research Methods

The research method adapted to address the specific research question in this study can be viewed from three dimensions those are the OBIA, FOTO and the AGB/carbon estimation based on field data. If looked from general point of view the methodological structure comprises the comparison of VHR satellite images and aerial photography from GE platform analysed through object based image classification (OBIA) and FOTO method for the respective remote sensing images to assess AGB

biomass and carbon of trees outside the forest in the study area. The step by step procedure is depicted in the flowchart below.

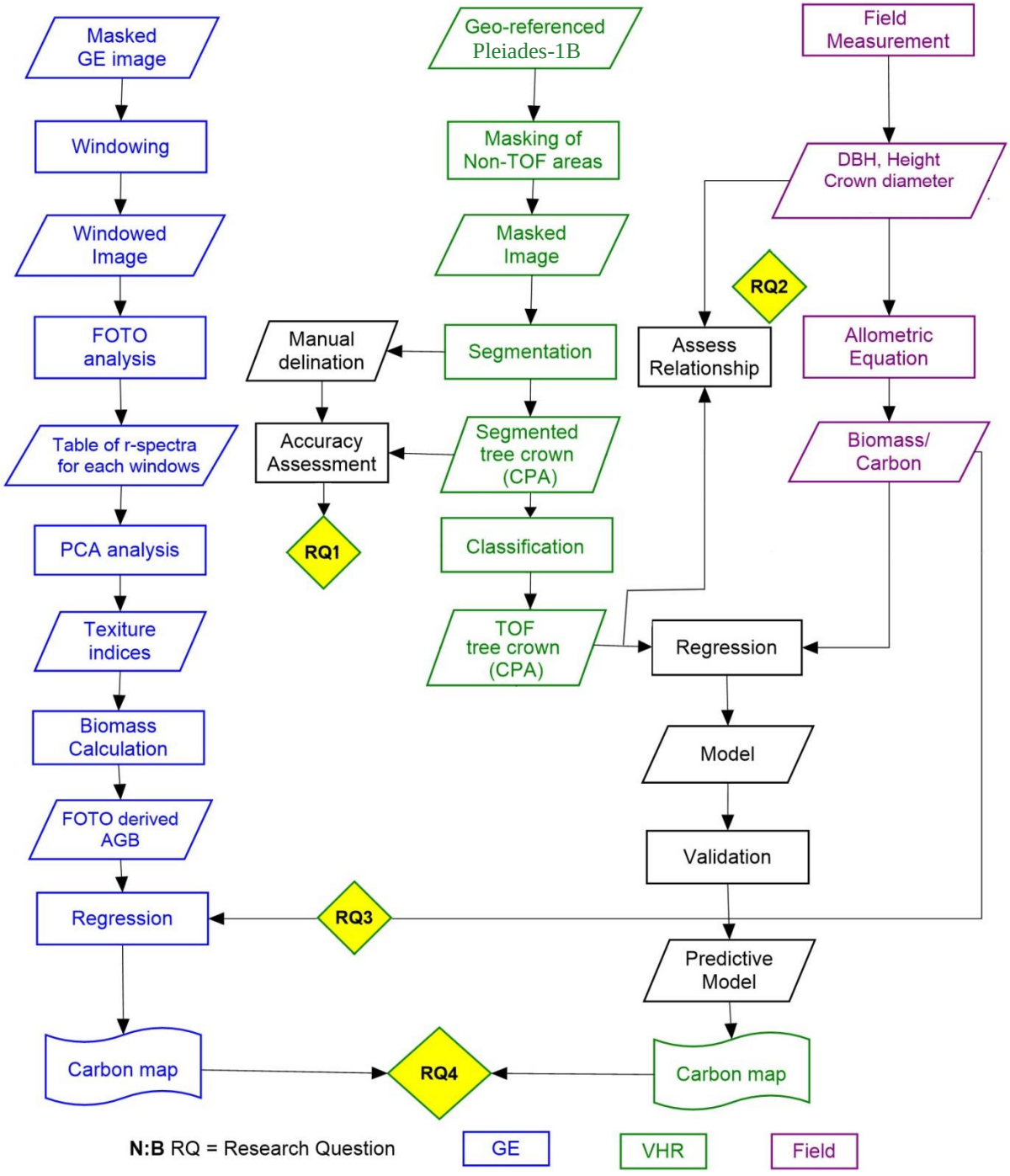

Figure 6. Flowchart of Research Methodology

3.3.1 Pan-sharpening of Pleiades-B1 image

There are a number of Pan-sharpening techniques available in different GIS software packages that enable to improve multispectral data using high spatial resolution panchromatic data. Among them are the Hue-Intensity-Saturation (HIS), Principal Components (PC) and High Pass Filter (HPF), Hyper-spherical color Sharpening (HCS), Gram-Schmidt (GS). Gram-Schmidt (GS) pan-sharpening method is the most accurate

and it's recommended for most applications (Maurer, 2013). Gram-Schmidt is usually more accurate because it uses the spectral response function of a given sensor to estimate what the panchromatic data look like therefore for this research Gram-schmidt (GS) is utilized for the purpose of pan sharpening Pleiades-1B image.

3.3.2 Visualization of TOF configurations in the study area

Visual image interpretation of TOF resources is frequently treated as the most important pre field work task. The GE platform represents a possibility for efficient visualization and mapping of TOF enabling a design of representative sampling scheme (Schnell et al., 2015). Visual image interpretation of TOF in the study area prior to the designing of sampling strategy supported practical selection of sampling units (Schnell et al., 2015). Furthermore preliminary classification of TOF elements into homogenous classes was done from visually analysing TOF elements in the landscape on the images in GE for an efficient and inclusive sampling scheme. Therefore visual photo interpretation was employed to study and to have an overview of the spatial pattern, configurations and distribution of TOF elements on the landscape.

3.3.3 Sampling Design

In assessing TOF there is always a trade-off between the size and number of sample plots to be used (Tomppo et al., 2011). However Schnell et al. (2015) suggests application of two- phase sampling strategy can be the most convenient way to address the above mentioned trade off. Two-phase sampling design is a sampling design where the sample selection is performed in two phases, where in the first phase the auxiliary variable x is observed and in the second phase the study variable y is observed. Hence the study applied this approach as follows:

1. Delineation of study area based on a RS data
2. Generation of the first-phase sampling units with TOF
3. Stratification of the first-phase sample units. Therefore TOF in the study area were stratified in to patches, standalone trees and tree lines based on the criteria of geometrical configuration
4. Determining the number of second-phase sample units, i.e. field plots for each stratum. The field sample units were allocated in proportion to the stratum importance and variance.

Therefore the research utilized the above mentioned strategy and a total number of 59 sample plots were surveyed to measure tree parameters.

3.3.4 Field data collection

Biophysical data

The field work was conducted between September and October 2016. The main objective for biometric field data collection was to gather information about tree parameters so that it can be used as a validation data for the methods that is executed in this research. To collect the appropriate field data different plots size and shape was used for each stratum. Typical plot sizes used for TOF assessment range from 150 m2 to 500 m2 for patches and 10 m (width) by 125 m (length) rectangular plots for tree lines where different linear tree configuration are considered as one class. However these thresholds can vary from place to place, and plot shape and size can be adapted in relation to specific area (Fridman et al., 2014). In this research according to the stratified map a circular sample plot of 300 m^2 was used for patches. Linear tree lines were break down into three strata for the purpose of sampling, hence for windbreak tree configuration a 25m length and a 5m width rectangular plot was laid, whereas for single and double tree lines along the road 5m*50m and 10m*50m rectangular plots was respectively taken.

Subedi et al. (2010) confirmed the use of GPS tracking as an efficient and accurate method for boundary location. Therefore iPAQ is used alongside printed maps obtained from GE to locate the various sample plots. Trees with DBH 10 cm or greater within a plot were only measured as trees less than 10 cm diameter contribute little to the AGB/carbon (Brown, 1997). Moreover tree height was measured from the tree base to the tip of the highest point using the Haga (refer to table 2). Furthermore name of the individual tree species and number of trees in each plot was recorded in the record sheet. All the collected field data were then compiled in excel file for further analysis.

3.3.5 Image segmentation of Pleiades-1B satellite imagery

The multi resolution segmentation process of the Pleiades-1B image has started by sub setting the image for developing a rule set prior to the segmentation of the whole image of the study area and selection of scale parameter.

3.3.5.1 Estimation of scale parameter

Scale parameter is an abstract value which defines the level of acceptable heterogeneity within a given image object during a segmentation process (Definiens, 2009). The choice of a scale parameter value in this research was first attempted by using the ESP tool. The ESP tool calculates the scale parameter by measuring the local variance (LV) as the mean of standard deviation (SD) of the objects for each object level obtained through segmentation. The rate of change in local variance (ROC-LV) per given iteration is then plotted against the increasing scale values consequently showing the optimum scale value were the image can be segmented successfully (refer figure 7).

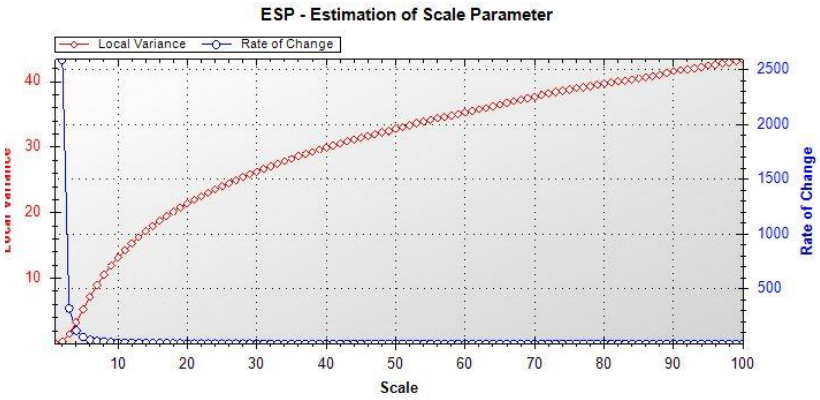

Figure 7. Estimation of scale parameter using the (ESP) tool

However the estimation of scale parameter using the ESP tool didn't yield a reliable value. Hence a subjective approach was employed and segmented polygons were visually inspected in a number of iterations before choosing scale parameter of 20 which was assumed to give ideal value for the segmentation of tree crowns both in linear and patch TOF configuration.

3.3.5.2 Multi-resolution segmentation

Object primitives where created after the scale parameter value was chosen by setting the threshold value for the homogeneity criterion parameters such as the shape and compactness. Different threshold values where attempted to observe how the variation in the values of homogeneity criterion parameters influence the accuracy of the segmentation process. Finally after several iterations and based on the visual evaluation of segmented polygons a scale parameter of 20 shape value of 0.9 and compactness/smoothness value of

0.8 was chosen as the suitable combination of thresholds for segmenting the Pleiades-1B imagery. Further details of the segmentation process can be found in figure 8 below.

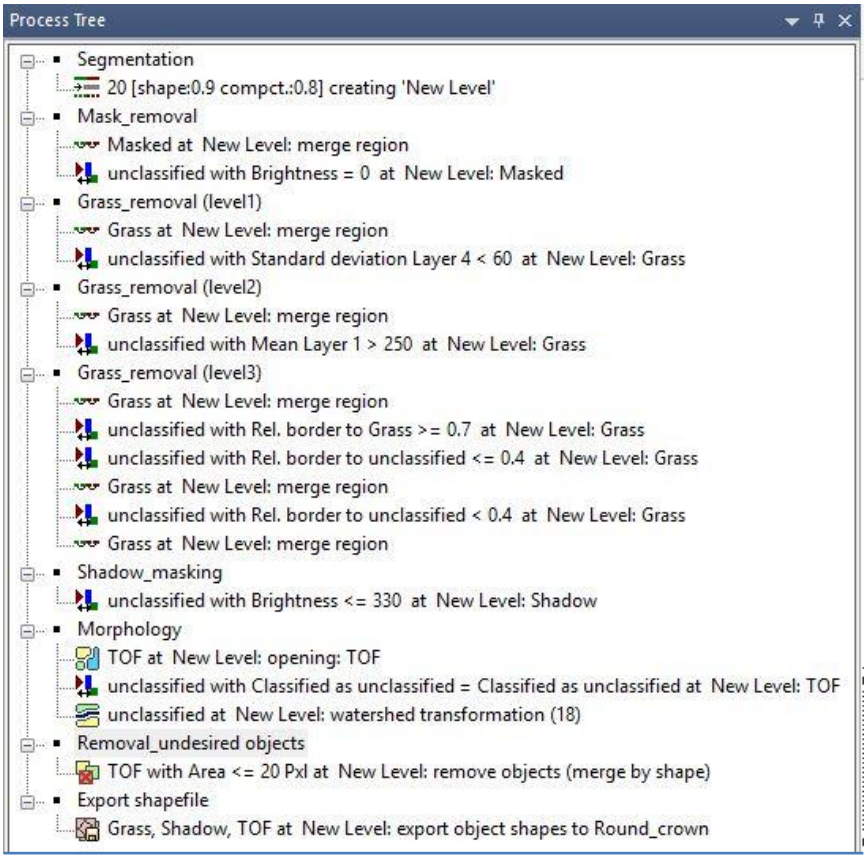

Figure 8. Multi-resolution segmentation rule set (workflow)

3.3.5.3 Watershed transformation & Morphology

Watershed transformation is an algorithm present in the eCognition software which is very useful in separating or dividing a group of intermingled tree crowns in to the ideal crown size observed in the image (Beucher, 1992). In the case of trees outside the forest intermingling of tree crowns is mainly observed in patch configuration however it was also observed though in a lesser extent in linear TOF configuration mainly in windbreaks. Hence the process of watershed transformation was very helpful in minimizing the problem of under-segmentation and splitting group of tree crowns in to individual tree crowns.

On the other hand morphology is the process of smoothing and enhancing the shape of a segmented image object so that it resembles its real world replica (Definiens, 2009). The morphology operation in eCognition has two options the open and closed image object. Open image object option eliminates pixels from within the image object in order to achieve smoothed figure. While on the other hand the closed option embraces similar neighboring pixels to fill the gap to achieve the desired shape. Moreover the mask option in the morphology algorithm gives a basis upon which image objects are replicated. In this research the open image object option was chosen with a very small circular mask to have minimal adjustment in the shape of TOF crowns.

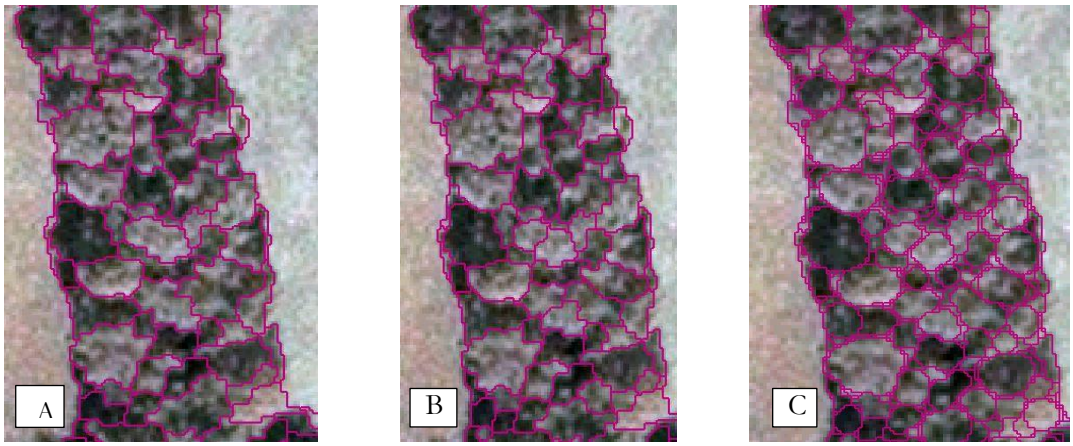

Figure 9. a) Multi-resolution *b) Watershed process* *c) Morphology process*

Refining of segmented polygons

Furthermore the relation to borders algorithm eCognition was utilized enormously in further refining the classification and removing of non TOF elements. The Relative border to (Rel. border to) algorithm in eCognition refers to the length of the shared border of neighboring image objects. The feature describes the ratio of the shared border length of an image object with a neighboring image object assigned to a defined class to the total border length (Definiens, 2009). If the relative border of an image object to image objects of a certain class is 1, the image Object is totally embedded in these image objects. If the relative border is 0.5 then the image object is surrounded 50% by polygons from a certain class and the remaining 50% from another class. Hence in this research the polygons which were misclassified as TOF where removed iteratively by changing the percentage of the border they share with the other non-TOF land cover classes. In the figure below, the red dashed circles indicate the removal of the polygons in the agricultural field which were misclassified as TOF.

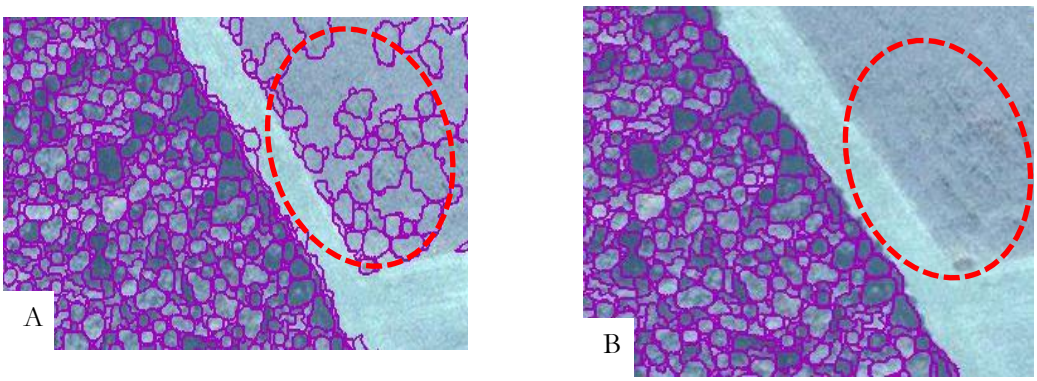

Figure 10. a) Before Rel.to border algorithm *b) After Rel.to border algorithm*

3.3.5.4 Segmentation accuracy assessment

Segmentation accuracy assessment is a procedure used to assess and evaluate the result of a segmentation process (Clinton et al., 2008). Accuracy assessment of segmented image objects is commenced to quantify the extent to which segmented image objects correspond with manually delineated training objects in terms of over-segmentation, under-segmentation and distance to a perfect match. Segmentation accuracy assessment prior to further image analysis is very essential because the segmentation result might influence

the consecutive processes that depend on the segmented image primitives. The quality of a segmentation result is closely linked image quality such as presence/absence of noise, spatial and spectral resolution as well as selection of segmentation parameters which supports the similarity of segmentation results with target objects (Clinton et al., 2008). In this study the segmentation accuracy of the image was assessed based on the comparison between the topological and geometric relationship of the segmented and manually delineated image objects. The topological relationship of image objects describe the "overlap" and "containment" of two image objects whereas the geometrical relationship stresses on the difference of object position (Möller et al., 2007). To assess the topological relationship of image objects an overlay function in GIS operation was used and segmented image objects were tested for their topological relationship with their respective reference objects (figure 11). Whereas geometrical relationships are assessed by measuring the distance from the center of a segmented object to the center of the manually delineated object.

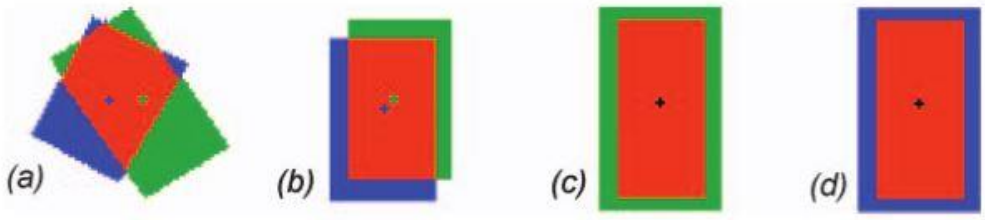

Figure 11. Topological relationship of segmented and manually digitized objects (Zhang, 1996)

Most empirical accuracy assessment methods quantify over segmentation and under segmentation based on the manually delineated objects to calculate the overall segmentation accuracy result. In this study to measure the over and under segmentation of segmentation process a set of manually delineated polygons referred as "x" were compared against segmented image objects referred as "y". Then over segmentation and under segmentation was calculated as follows.

$$\text{Over segmentation} = 1 - \frac{\text{Area } \{X \cap Y\}}{\text{Area } \{X\}} \quad \text{---------- Equation 1}$$

$$\text{Under segmentation} = 1 - \frac{\text{Area } \{X \cap Y\}}{\text{Area } \{Y\}} \quad \text{---------- Equation 2}$$

Finally the under-segmented and over-segmented value was used to calculate the goodness of fit of the segmented polygons. The goodness of fit is measured by the distance index "D" the distance index is calculated based on the over and under segmentation result and its value ranges from 0 to 1, where 0 is a perfect match and 1 is the minimum mismatch tolerated.

$$D = \frac{\sqrt{\text{over-segmentation} + \text{under-segmentation}}}{2} \quad \text{---------- Equation 3}$$

According to Zhan et al. (2005), another evaluation of segmentation accuracy is the 1:1 matching where it measures the enclosure a segmented and digitized polygon. A 50% overlap of a digitized and segmented polygon is acceptable and the polygons are assumed to have a 1:1 correspondence. Hence this measure was also used for this study to evaluate the 1:1 correspondence between segmented and manually delineated objects.

3.3.6 FOTO method

The FOTO method starts by masking all land cover classes which are not of genuine interest to the study. However the study area in this research is characterized by numerous scattered agricultural fields which don't have a regular occurrence pattern. Therefore only forest areas that are not considered as TOF are masked out to eliminate over estimation of TOF AGB/carbon. Therefore all the non TOF land cover classes are identified based on the R-spectrum curves and frequency peaks they yielded and removed from the principal component analysis for developing texture indices to predict AGB/carbon of TOF in the study area.

3.3.6.1 Windowing

The proceeding step is windowing of the GE image in to equal size grids in which each window should include several repetitions of the largest crown diameter of minimum 5 to 7 trees (equation 4). Choosing the correct window size is critical and important as the 2DFFT function in MATLAB captures the repetition in the canopy gradient with in each specific window. However for this study area it was difficult to find a window value that constitutes only of a continuous tree canopy, almost all windowed grids in the image contain non-TOF land cover classes mainly agricultural fields and grasslands (see figure 12). Moreover Linear TOF configuration was eliminated from the textural analysis as windowing the image in to window sizes that correspond with the plot size used for field data measurement of linear TOF configuration was so difficult to be implemented in the FOTO analysis.

The window size is expressed in meters where window size (WS) is:

$$WS = N.\Delta S \quad \text{----------} \quad \textit{Equation 4}$$

Where N is the number of pixels in X or Y direction and ΔS is the pixel size in meters (Proisy et al., 2011).

Figure 12. Windowed aerial photography from Google Earth

3.3.6.2 2Dimensional Fast Fourier transform (2DFFT)

After windowing the image in to equal size grids the windowed image was subjected to the 2DFFT transformation method in MatLab for the computation of the r-spectra table. The table of r-spectra gives

the frequency distribution for the repetitive pattern of forest canopy with in a given window. The r indicates the number of times that a pattern in this study it can be a tree crown or a continuous field of grass or a building whatever happens to be in any given window repeats itself . Therefore an image with a coarse texture gives a radial spectrum which is tilted toward low frequencies; while fine texture more or less balanced spectra

3.3.6.3 Principal component analysis (PCA)

The acquired r-spectra table which is mainly the table of frequency in cycles/km for every given window in the image is submitted for PCA analysis for ordination and standardization. PCA is executed to standardize or ordinate the column frequency values considering it as a quantitative variable. The PCA enables an overall comparison between textural profiles of each and every window in the image expressed in cycles/km hence the windows having similar textural profiles are characterized by similar PCA scores and vice versa (Proisy et al., 2007). Out of all the computed 'PCA scores' the prominent axes which explain more than 70% of the textural variation in the image are chosen as texture indices (TC) for predicting AGB/Carbon. In many studies the first three PCA axes are chosen as texture indices for predicting AGB/carbon because this TC define the majority of the variation observed in the image. Moreover these first three TC have proven to show good correlation with field estimated AGB (Proisy et al., 2007).

In this research the ordination of the frequency table(r-spectra table) was performed using the principal component analysis (PCA) present in SPSS. Only frequencies ranging from 50 cycles/km up to 450 cycles/km were considered for standardization using PCA to be used for further textural analysis because frequency other than this ranges belong to other land cover classes of the study area. The three first factorial principal axes (PCA) accounted for more than 73% of the total variability. Therefore this PCA which hereafter will be referred as texture indices (TC) values were chosen to be used as predictors for AGB. Hence the three TC scores for each window in the image were calculated.

3.3.7 Above ground biomass (AGB) and carbon stock calculation based on field data

Biomass estimation based on allometric equations are developed by establishing a relationship between the various physical parameters of the trees such as the diameter at breast height, height of the tree trunk, total height of the tree, crown diameter, tree species, etc. (DeFries et al., 2007). Most allometric equations for AGB biomass calculation involve diameter at breast height (DBH) and tree height (H) and sometimes a combination of both as explanatory variable. However according to a study by Zianis & Seura (2005), most AGB calculation either solely depend on diameter at breast height (DBH) values alone or use tree height as second explanatory variable. This situation is mainly attributed to the fact that height measurements can be less accurate and subjected to human induced apparent errors and might introduce discrepancy in final AGB calculation. In addition to that allometric equations which are specifically designed for the purpose of AGB estimation of TOF is hard to find (Schnell, 2015). Therefore in this study the general equation which is proposed by IPCC for calculating AGB biomass and quantification of carbon will be used to assess the AGB and carbon stock of the study area (citation).

$$Y = 0.5 + [(25000 \bullet (DBH)\ 2.5) / ((DBH2.5) + 246872)] \text{ ----------} \quad \textit{Equation 5}$$

Where,

Y= aboveground dry matter, kg (tree)-1

DBH =diameter at breast height

Carbon stock is calculated once the biomass is calculated using the conversion factor proposed by IPCC (IPCC, 2003)

$$C = B * CF \quad \text{---------- Equation 6}$$

Where,
C: carbon stock (Mg/C)
B: dry biomass
CF: carbon fraction of biomass (0.47)

3.3.8 Regression analysis and model validation

Regression analysis was used to assess the relationship between the dependent and the independent variables and to develop a predictive model for AGB and carbon estimation. The predictive variables for the AGB and carbon estimation derived from remotely sensed data using both methods include the crown projection area (CPA) and texture indices. The field data were divided into training and testing datasets. For the estimation of AGB/carbon of TOF based on OBIA out of the total number of trees which has showed 1:1 correspondence with manually delineated tree crowns 70% were used as training data set to develop models and the remaining 30% of the data set for model validation (Foody, 2003). The same procedure was employed in the regression analysis of AGB/carbon estimation based on the FOTO method. Were 70% of the patch sample plots where used for model development and the remaining 30% was used for model validation. The performance of the model was evaluated by using a Root Mean Square Error (RMSE) and coefficient of determination (R^2). To calculate the RMSE, the values of observed (field data) and predicted (derived from the model) were compared using the equation below

$$RMSE = \sqrt{\frac{1}{n}\sum_{i}^{n}(Yp - Yo)^2} \quad \text{---------- Equation 7}$$

Where,
RMSE = Root mean square error
Y p = predicted
Y o = observed
N = number of observations

3.3.9 AGB and Carbon Mapping

Using the best fit prediction model AGB of the study area will be calculated and then carbon which is 0.47 of AGB (IPCC, 2006) will be calculated and two maps from VHR and GE will be generated. Comparison of the coefficient of determination (R^2) of the VHR and GE will be compared to assess the estimation of carbon from the two very high resolution imageries.

4. RESULT

4.1. Descriptive analysis of field data

Descriptive statistics is introduced to describe the patterns, spread and characteristics of the field collected data. The pie chart below depicts the total percentage of trees observed in patches, windbreaks, single tree lines along roads and double tree lines along roads.

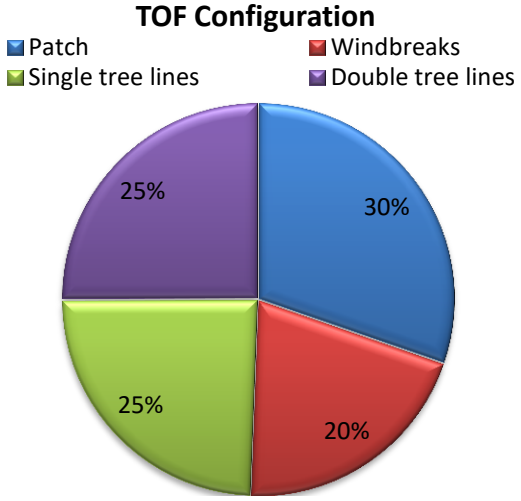

Figure 13. Pie- chart percentage of trees sampled for different TOF configurations

The tables below illustrate a descriptive summary of the overall tree DBH and Height measured in the field for the different TOF configurations. As table 4 indicates patches have the lowest men DBH and single tree lines along the roads have the highest mean DBH. In addition to that all the DBH measurements in all TOF configurations are skewed to the right though the degree of skewness varies.

Table 4. Statistical summary of DBH measurement in the different TOF configuration

	N	Minimum	Maximum	Mean		Std. Deviation	Variance	Skewness	
	Statistic	Statistic	Statistic	Statistic	Std. Error	Statistic	Statistic	Statistic	Std. Error
Double lines along roads_DBH	148	11.0000	90.0000	32.824324	1.3153452	16.0018648	256.060	1.378	.199
Patch_DBH	179	10.5000	66.5000	23.906145	.8838788	11.8254922	139.842	1.532	.182
Single tree line_DBH	144	12.0000	72.0000	38.298611	1.2990138	15.5881656	242.991	.440	.202
Windbreak trees_DBH	120	11.0000	75.0000	35.085833	1.3662664	14.9666986	224.002	.113	.221
Valid N (listwise)	120								

Table 5 indicates a statistical summary of height measurement in the different TOF configurations. As it can be observed from the table trees in patches were found to have the highest mean height followed by windbreak trees, single tree lines along the roads and double tree lines along the roads.

Table 5. Statistical summary of height measurements in different TOF configurations

Descriptive Statistics

	N	Minimum	Maximum	Mean		Std. Deviation	Variance	Skewness	
	Statistic	Statistic	Statistic	Statistic	Std. Error	Statistic	Statistic	Statistic	Std. Error
Double tree lines_height	148	5.0	20.0	11.845	.2922	3.5542	12.632	.802	.199
Single tree lines_height	132	1.0000	26.0000	14.103030	.3727394	4.2824502	18.339	.039	.211
Windbreak trees_height	120	4.5	26.0	15.722	.5106	5.5935	31.287	.041	.221
Patch_height	179	10.0000	32.0000	22.063128	.3700352	4.9507329	24.510	-.165	.182
Valid N (listwise)	117								

Moreover as the box plot for DBH in the different configurations indicates the measurements were characterized by uneven spread from the second quartile (median) of the observations and more outliers were found in patch configuration TOF as compared to the other TOF configurations.

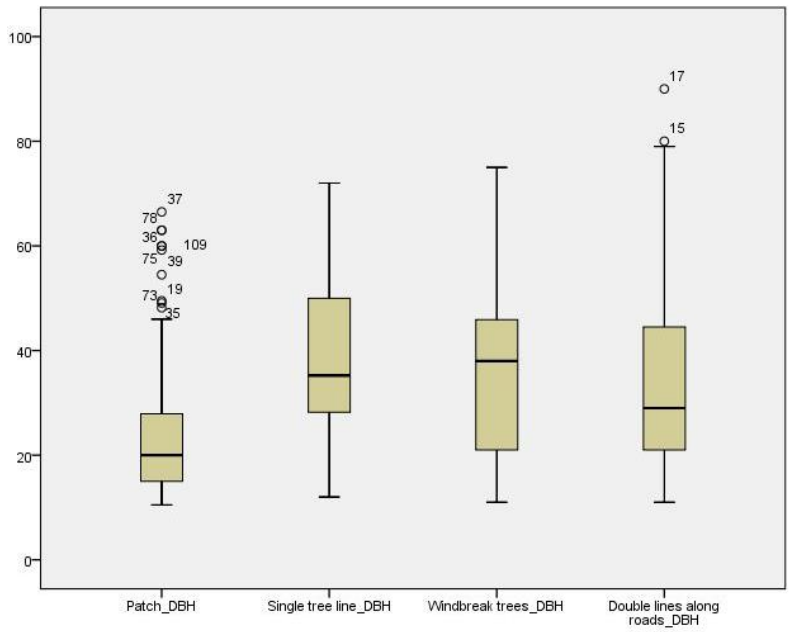

Figure 14. Boxplot of different TOF configurations DBH

A normality test was also done to examine the distribution of for the DBH and height measurement of trees in the study area, and it was found that both DBH and height measurement are not normally distributed. The normality test through both the Kolmogorov- sminrov and the Shapiro-wilk method has indicated both measurements have a p value < 0.05 at 569 degrees of freedom.

Table 6. Normality test result of DBH and Height measurements

Tests of Normality

	Kolmogorov-Smirnov[a]			Shapiro-Wilk		
	Statistic	df	Sig.	Statistic	df	Sig.
DBH	.114	569	.000	.931	569	.000
Height	.120	569	.000	.965	569	.000

Throughout the 59 sample plots 7 dominant tree species where identified in the study area. Dominance and occurrence of tree species vary per configuration. In patch TOF configuration the most dominant tree species include, *Betula pendula* (birch), *Fagus sylvatica* (beech) and *Quercus robur* (oak), however *Populus* (poplar) and *Pinus sylvestris* (scots pine) are also found in few numbers. In the linear formation trees especially in double and single tree lines along the roads *Quercus robur* (oak) constitute the highest percentage. In windbreaks *Quercus robur* (oak) are also the most reoccurring tree species followed by *Fagus sylvatica* (beech) and *Betula pendula* (birch) see figure 15.

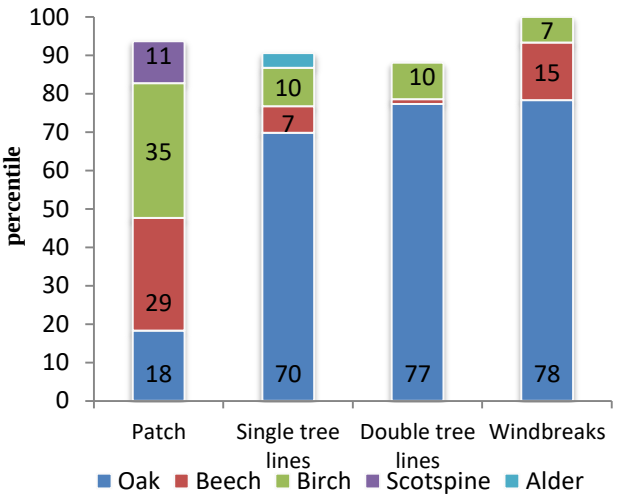

Figure 15. Percentage of different tree species in different classes

Paired t-test of mean DBH measurements between different TOF configurations

The paired samples t-test was conducted on SPSS to test whether there is a significant difference in tree DBH measurements in the different TOF configurations. In other words to the test of significance was done to observe weather mean tree DBH measurements vary significantly among the different TOF configurations. First the test was done to evaluate whether there is a significant difference in the classes of the linear configuration TOF namely, windbreaks, double tree lines along roads and single tree lines along the roads. According to the result of the test DBH measurements among all the linear formations trees has shown no significant difference with a p value > 0.05 (table 7) at 95% confidence level. Whereas DBH measurement in patches and DBH measurement in the linear formation trees collectively has showed a significant difference at a p value equal to zero at 95% confidence level (table 8).

Table 7. Paired sample test of the three classes in linear configuration trees

Paired Samples Test

		Paired Differences					t	df	Sig. (2-tailed)
		Mean	Std. Deviation	Std. Error Mean	95% Confidence Interval of the Difference Lower	Upper			
Pair 1	DBH_db - DBH_sl	-4.0916667	25.4207306	2.3205846	-8.6866559	.5033226	-1.763	119	.080
Pair 2	DBH_Wb - DBH_sl	-3.4308333	21.4654023	1.9595142	-7.3108671	.4492004	-1.751	119	.083
Pair 3	DBH_db - DBH_Wb	-.6608333	22.0279322	2.0108659	-4.6425486	3.3208820	-.329	119	.743

Table 8. Paired sample t test among DBH of trees in patches and linear formation TOF

Paired Samples Test

		Paired Differences					t	df	Sig. (2-tailed)
		Mean	Std. Deviation	Std. Error Mean	95% Confidence Interval of the Difference Lower	Upper			
Pair 1	DBH_patch - DBH_linear	-26.0256983	16.4281585	1.2278982	-28.4488092	-23.6025874	-21.195	178	.000

4.2. Multi-resolution segmentation

Multi-resolution segmentation was done on the Pleiades-1B very high resolution satellite imagery to generate CPA for the estimation of AGB/carbon of TOF, the step by step work flow of the multi-resolution segmentation process can be observed from the rule set in figure 16.

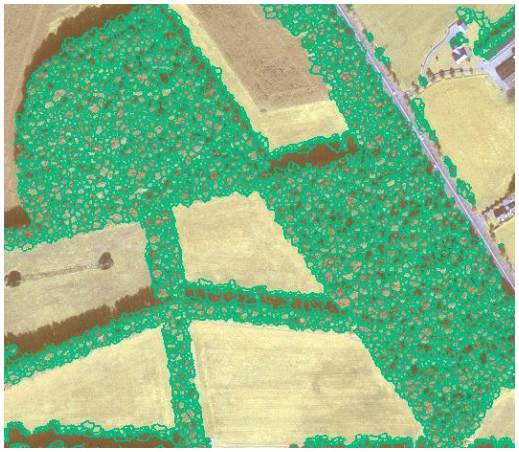

Figure 16. Illustration of the final output of the multi-resolution segmentation process in eCognition

4.3. Segmentation validation

The segmentation accuracy for the multi resolution segmentation of the high resolution satellite imagery was done by comparing the segmented image with a 120 manually delineated tree crowns to address research question one. Most segmentation accuracy assessments are based on two approaches i.e. measure of goodness of fit through "D" value calculation and 1:1 matching of segmented and digitized polygons (see figure 17). For this segmentation a "D" value of 0.28 was attained that is equivalent to 78% goodness of fit accuracy value. In addition to this, the 1:1 matching of the segmented and reference polygons was used and out of 110 polygons 78 polygons (which accounts to 71%) were found to have a 1:1 correspondence with the digitized polygons area overlapped greater than 50% with the reference polygons. Hence the overall segmentation accuracy is 72% where over-segmentation of segmented polygons is more pronounced than under-segmentation of segmented polygons.

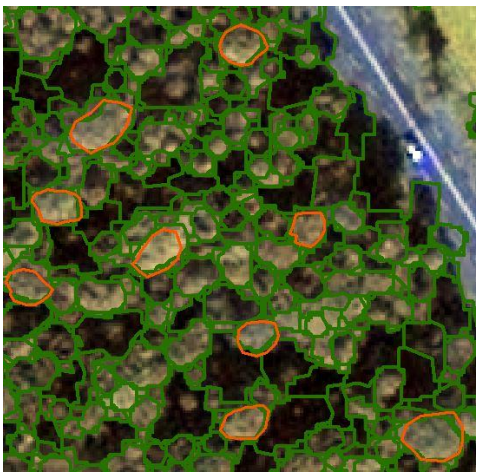

Figure 17. Comparison of segmented and manually digitized polygons

4.4. AGB/carbon modelling based on OBIA

After the analysis of the Pleiades-1B satellite imagery using OBIA method a model for calculating TOF AGB/carbon in the study area was developed by using CPA as predictive variable. The significance analysis between the DBH measurement of patch and linear TOF configuration has proved there is significant difference in DBH measurements between the two configurations (table 8). Moreover the relationship between DBH and CPA has shown a strong correlation in linear configuration trees (R^2=0.89) as compared to the trees in patches (R^2=0.78). Therefore it was assumed to be practical to assess the AGB/carbon of linear TOF configuration and patches separately to avoid biasness and error in the estimation of AGB/carbon. Hence separate models were developed for linear configuration trees and patches.

4.4.1. Relationship between DBH and CPA of linear and patch configuration TOF

The figures below illustrate the correlation between DBH and CPA of trees in patches and linear TOF configuration to address research question 2. In figure 18a the segmented CPA polygons have showed good correlation with field measured DBH at an R^2 = 0.88 at 95% confidence level in linear TOF configuration. This can mainly be due to a lesser presence of tree intermingling witnessed in linear configuration in which this in turn has resulted in more accurate CPA segmentation of linear TOF configuration than patch TOF configuration. On the other hand diagram 18b demonstrates the relationship between CPA and DBH if patch configuration TOF which was observed to be smaller than linear TOF configuration at R^2 = 0.79 at 95% confidence level.

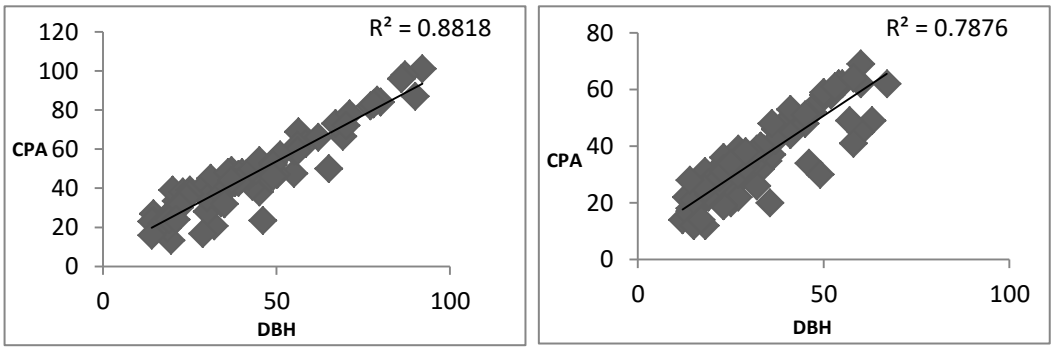

Figure 18. a) Scatter plot of CPA & DBH of linear configuration b) Scatter plot of DBH & CPA of patch configuration

4.4.2. Model development

4.4.2.1. Modelling carbon from CPA in linear TOF configuration

A number of 50 trees were selected from the 80 trees in the linear formation trees which have shown a 1-1 matching for model development. Subsequently the model was developed based on the regression analysis conducted by assessing the relationship of Carbon which is assumed as dependent variable and CPA which is the independent variable. A non-linear polynomial relationship has generated a strong relationship between carbon and CPA of linear formation trees at 95 % confidence level. Moreover the ANOVA test performed to analyse whether there is significant difference between mean carbon in kg and mean CPA has proved there is no significant difference which further supports the relationship between segmented CPA and carbon. According to the R^2 value obtained the 82% of the variation in carbon measurement is explained by CPA (see figure 19).

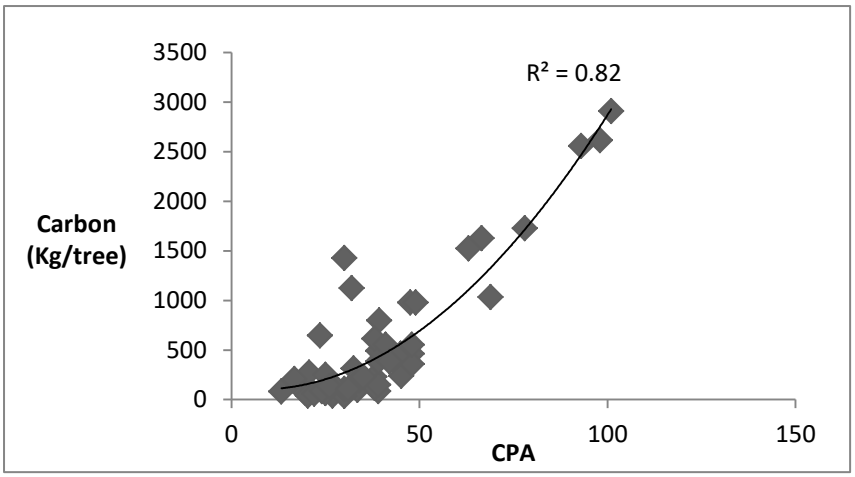

Figure 19. Scatter plot of carbon and CPA

Carbon = 0.319CPA² - 4.4359CPA + 116.7---------- *Equation 8*

The one-way ANOVA conducted to verify the significance of the obtained R² value also confirms that the regression analysis was significant at 95% confidence level. Below is a table of summary of the regression analysis and the ANOVA test (see table 9).

Table 9. Result of regression analysis of linear formation trees

	Coefficients	*Standard Error*	*t Stat*	*P-value*	*Lower 95%*	*Upper 95%*	*Lower 95.0%*	*Upper 95.0%*
Intercept	116.6463861	226.6539321	0.514645323	0.609319503	-339.8580666	573.1508389	-339.85807	573.1508389
X Variable 1	-4.43593815	9.409028499	-0.47145549	0.639593343	-23.38669434	14.51481804	-23.386694	14.51481804
X Variable 2	0.319651734	0.082406531	3.878961147	0.000339201	0.153676459	0.485627008	0.15367646	0.485627008

ANOVA					
	df	*SS*	*MS*	*F*	*Significance F*
Regression	2	19372726	9686362.9	109.3286023	5.29529E-18
Residual	45	3986938	88598.617		
Total	47	23359664			

Regression Statistics	
Multiple R	0.91067219
R Square	0.829323837
Adjusted R Square	0.82173823
Standard Error	297.6551979
Observations	48

4.4.2.2. **Modelling carbon from CPA in patch TOF configuration**

The regression analysis to assess the relationship among CPA and carbon of trees found in patches was conducted to analyse how much the predictive variable which is CPA is in agreement with the response variable which is carbon measured in kg. A polynomial function predictive model was fitted to calculate carbon based on a remote sensing data using a number of 65 trees out of 95 trees which were able to be recognized in the image and which has shown a 1:1 matching with the digitized tree crowns.

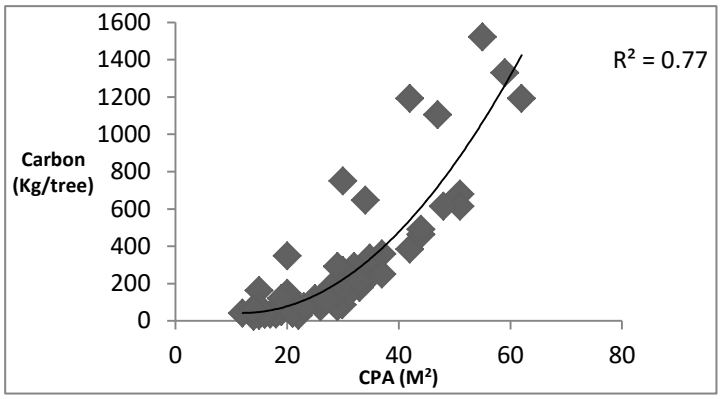

Figure 20. Scatter plot of CPA and Carbon of trees on patches

Carbon = $0.5511CPA^2 - 13.13CPA + 120.6$ ---------- *Equation 9*

The R^2 which is the statistical measure of goodness of fit of the independent and dependent variable was found to be 0.77 for trees which are considered as TOF located in small patches. The significance of the obtained R square has a P value > 0.05 which is statistically significant. Moreover it was observed that the obtained R^2 for trees which are found in patches is lower than the R^2 obtained for trees which are found in linear formation configuration. The table of the summary statistics of the regression model along with the result for the ANOVA test is presented below (table 10).

Table 10. Summary of regression analysis for patches

	Coefficients	*Standard Error*	*t Stat*	*P-value*	*Lower 95%*	*Upper 95%*	*Lower 95.0%*	*Upper 95.0%*
Intercept	120.670797	137.4493693	0.877929	0.383427	-154.1762036	395.517798	-154.1762	395.5178
CPA	-13.13420507	8.705370172	-1.508747	0.136526	-30.54166858	4.27325845	-30.54167	4.2732584
CPA^2	0.551054915	0.12446381	4.427431	4.02E-05	0.302174145	0.79993569	0.3021741	0.7999357

ANOVA

	df	*SS*	*MS*	*F*	*Significance F*
Regression	2	5698365.518	2849183	103.6879	2.3762E-20
Residual	61	1676184.721	27478.44		
Total	63	7374550.239			

SUMMARY OUTPUT

Regression Statistics	
Multiple R	0.879037459
R Square	0.772706854
Adjusted R Square	0.76525462
Standard Error	165.766215
Observations	64

4.4.3. **Model Validation**

4.4.3.1 Model Validation of linear TOF configuration

The predicted carbon in kg/tree which was calculated through the best fitting model was plotted against the carbon calculated using the AGB conversion factor. For validating the predictive model 30 sample tree crowns which remained from the model development were used. The R^2 obtained from the validation

model was 0.89 meaning that the predicted carbon is 89% in agreement with the observed carbon. More over the RMSE was calculated to assess the relative error in carbon measurements between the predicted and observed carbon and it was found to be 27%.

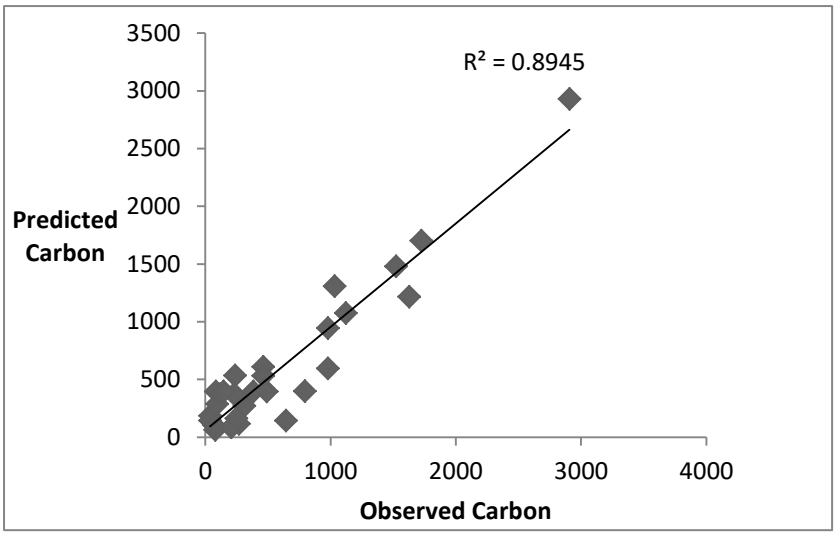

Figure 21. Scatter plot of model validation for linear formation TOF configuration

4.4.3.2 Model Validation of Patch configuration TOF

Similarly the predicted carbon in kg/tree was plotted against the observed carbon in patch configuration of trees outside the forest. Both the R^2 as well as the RMSE was calculated to assess the statistical measure of goodness of fit and how carbon calculated from the remote sensing data is in agreement with the carbon measured from the field. The R^2 for the fitted validation model was obtained to be 0.82 meaning that carbon calculated based on remotely sensed variable CPA has 82 % agreement with carbon calculated from the field. Moreover the RMSE value calculated has also indicated that there is a 34% relative error or discrepancy in the measurement of carbon predicted from the remote sensing data when compared with the field calculated carbon.

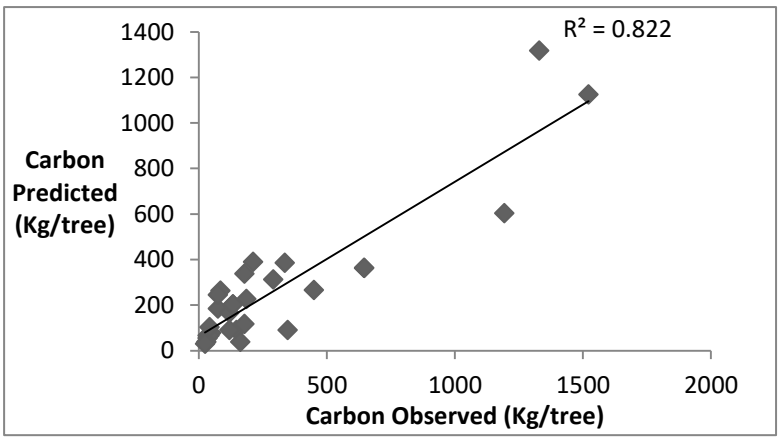

Figure 22. Scatter plot of model validation for Patch TOF configuration

4.4.4. Carbon stock mapping of linear and patch TOF configuration

the carbon stock mapping was done separately for linear formation trees and patches based up on the fact that a significant difference has been discovered both on DBH measurement of trees on patches as well as

on linear TOF configuration. Moreover according to the correlation test done the relationship between CPA and DBH in linear TOF configuration and patch TOF configuration was also found to be different based on the calculated correlation coefficients.

CPA which was obtained using a multi-resolution segmentation in eCognition was used as a predictive variable for AGB/carbon estimation. Therefore a separate model was developed for the two individual classes and the developed models where validated through field calculated carbon which is mentioned as observed carbon. The map below demonstrates the OBIA method generated carbon stock map of linear TOF configuration with reasonable accuracy (this addresses research question number 4).

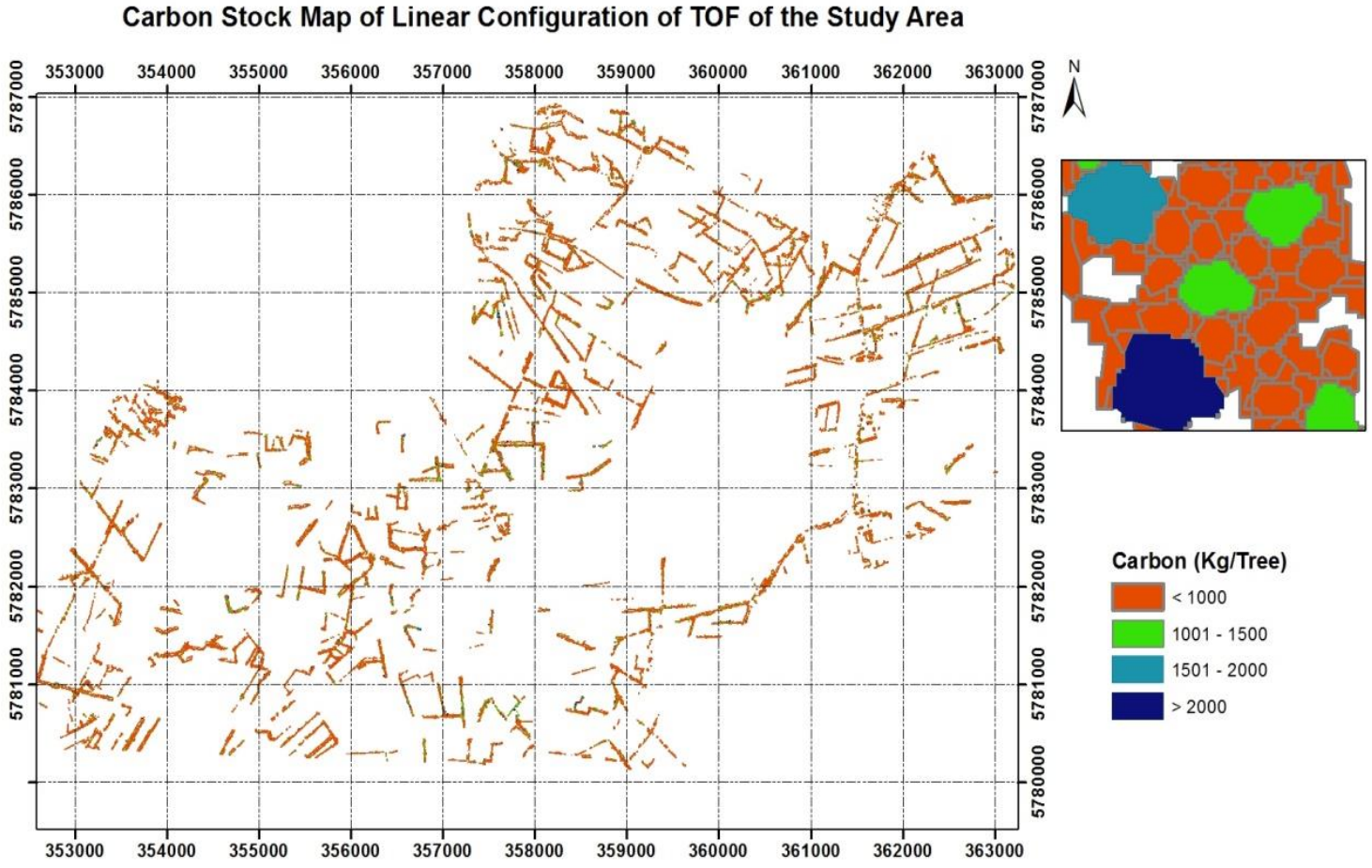

Figure 23. Carbon Stock Map of Linear Configuration of TOF of the Study Area

Similarly the map below demonstrates the OBIA method generated carbon stock map of patch TOF configuration with reasonable accuracy.

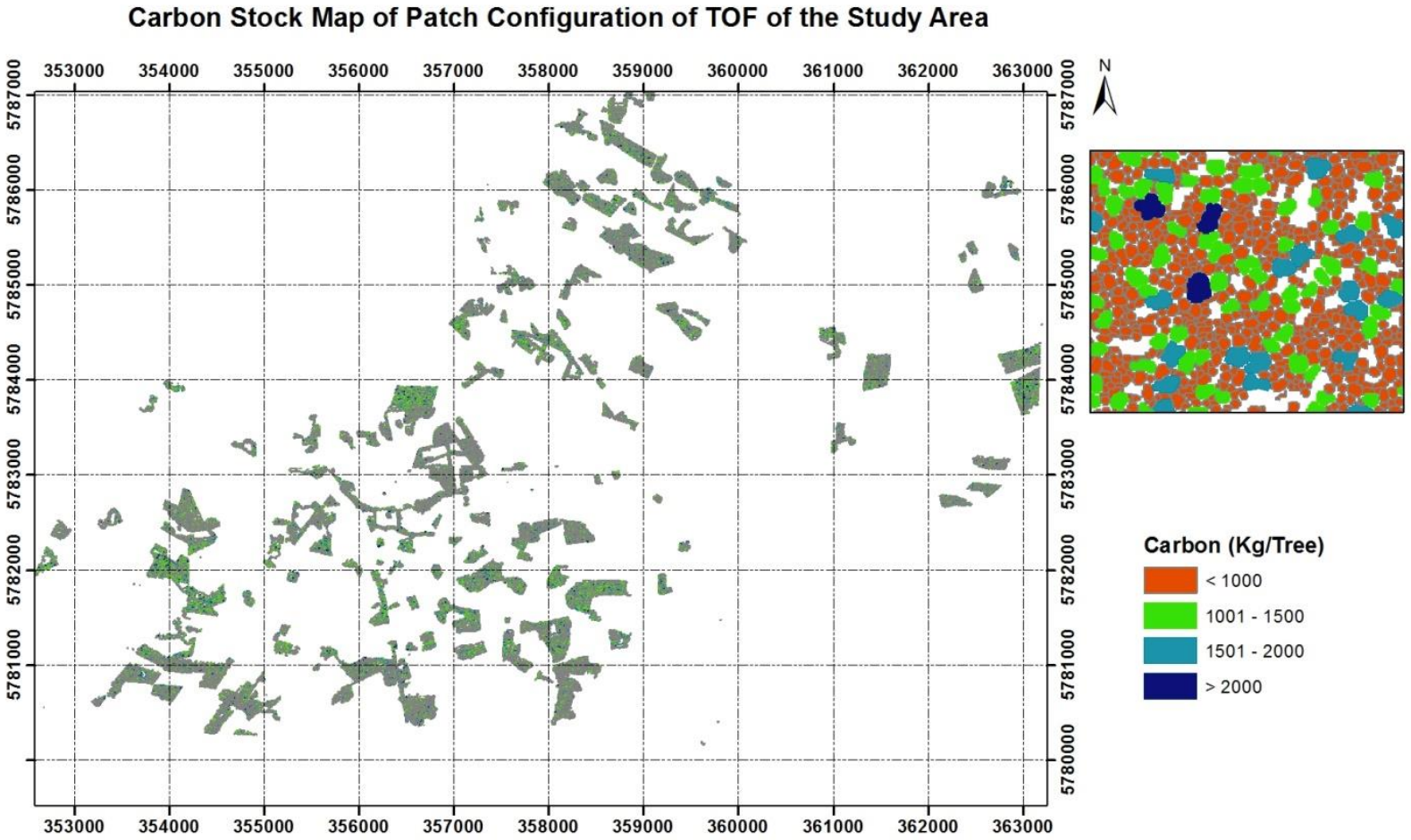

Figure 24. Carbon Stock Map of Patch Configuration of TOF of the Study Area

4.5 Modelling of AGB/carbon based on FOTO derived texture indices

According to the principal component analysis conducted to identify the most prominent texture indices that explain the highest variation in the image the first three axes where chosen as texture indices (TC) for AGB/carbon estimation. Therefore the first three principal components of the r-spectra table explained 73% of the total variation in the high resolution GE imagery. Therefore these FOTO texture indices were considered as predictive variables for AGB/carbon estimation. The FOTO based AGB/carbon prediction model was calibrated using a linear multiple regression model between the TC as independent variables and field plot AGB/carbon as dependent variable.

The scatter plots in figure 25 allow a comparison of field measured carbon and FOTO measured carbon to respond to research question 3 of this research. From the scatter plot it can be observed that 68% of the FOTO measured carbon is in agreement with the field measured carbon in patch configurations with R^2 value of 0.68 and RMSE value of 39%.

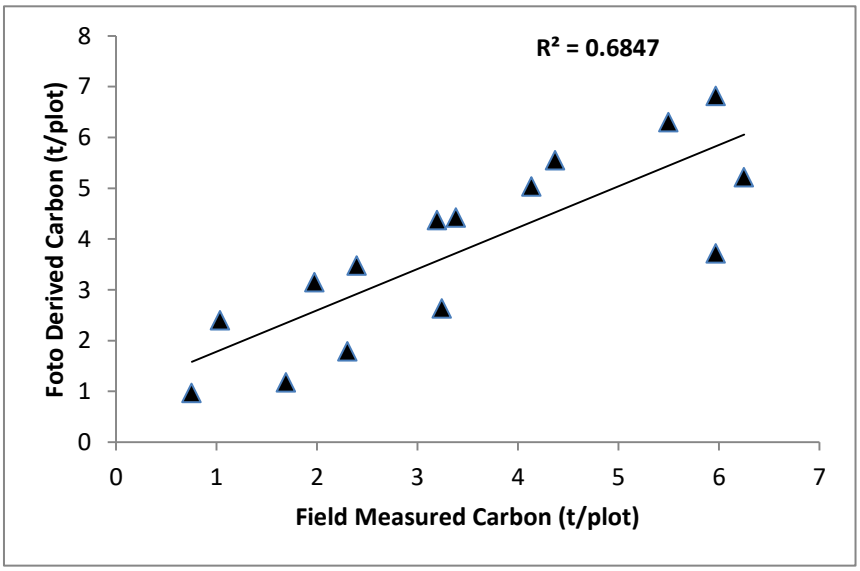

Figure 25. Scatter plot of FOTO carbon estimation validation

4.5.1 Carbon stock mapping based FOTO

Finally the validated model was used to calculate carbon in tons/plot using the three texture indices which were considered as predictive variables. The AGB/carbon estimation was performed using multiple linear regression models by means of the three textural indices (scores of the three main PCA axes) as independent variables. Figure 26 depicts the final carbon map produced using the FOTO method, the carbon map has a spatial resolution which is equal to the window size used for the purpose of the 2D FFT approach in MatLab, which 20m*20m therefore the spatial resolution of the map is courser as compared to the original aerial photography from GE. The map below demonstrates that the FOTO method yielded carbon stock map of TOF with reasonable accuracy (this addresses research question number 4).

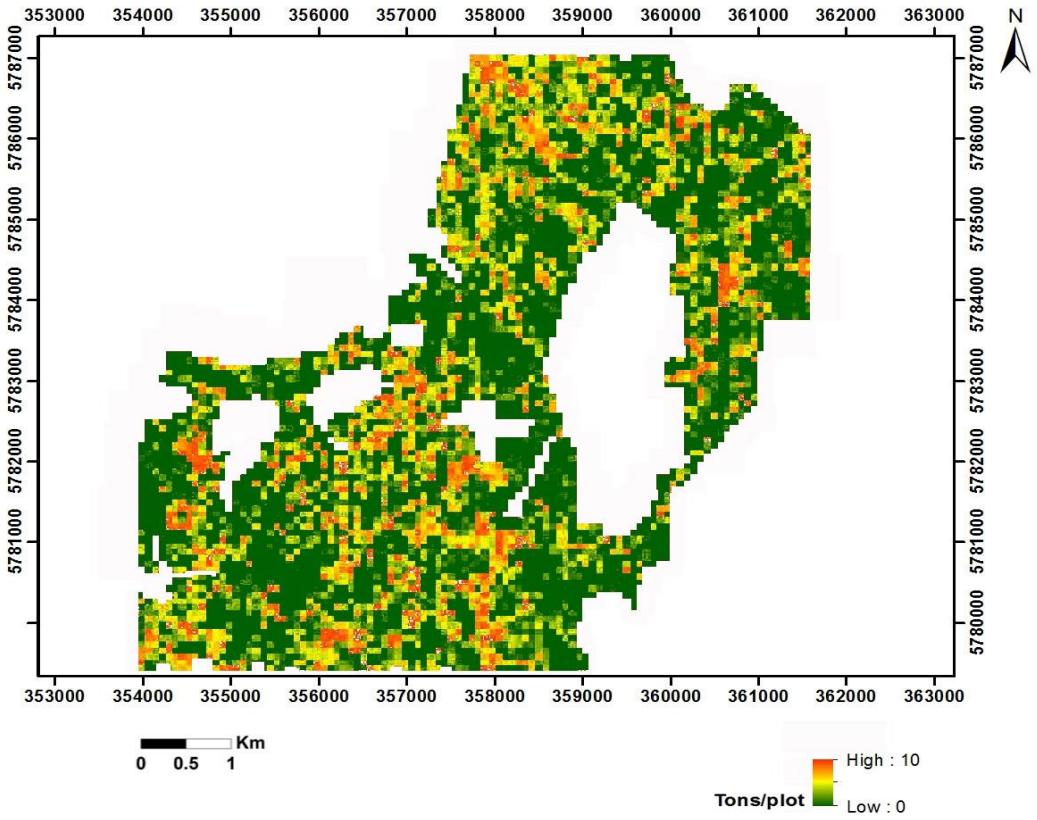

Figure 26. FOTO Derived Carbon Stock Map of Patch Configuration of the Study Area

4.6 comparison of FOTO and OBIA method in TOF AGB/carbon estimation

The carbon derived from the Pleiades-1B estimation using the OBIA method was compared with the carbon estimated from aerial photography from GE using FOTO method for patch TOF configuration based on the field measured AGB/carbon. Since AGB/carbon estimation based FOTO method for linear TOF configuration was found to be not applicable the comparison is for patch configuration TOF only.

The performance of the two methods is estimated based on how the predicted carbon value from the two methods is close to the field measured carbon based on the two estimators of goodness of fit that is R^2 and RMSE value. According to the coefficient of determination obtained for the prediction of carbon from OBIA and FOTO for patch configuration TOF that is R^2=0.82 and R^2=0.68. The OBIA was observed to better explain the variation between field measured and predicted carbon in both linear and patch TOF configuration with higher coefficient of determination value (0.82) and lower RMSE (34%).

In addition to that a correlation test was done to assess the significance of the relationship between field measured AGB/carbon and FOTO predicted carbon and OBIA predicted carbon. Hence the correlation test indicates that both FOTO predicted carbon and OBIA predicted carbon has significant relationship with field measured carbon but with different correlation coefficient (see table 11 & 12 below).

Table 11. Pearson correlation test between field measured carbon and OBIA predicted carbon

		Carbon_field observed	Carbon_OBIA predicted
Carbon_field observed	Pearson Correlation	1	.907**
	Sig. (2-tailed)		.000
	N	29	29
Carbon_OBIA predicted	Pearson Correlation	.907**	1
	Sig. (2-tailed)	.000	
	N	29	29

**. Correlation is significant at the 0.01 level (2-tailed).

Table 12. Pearson correlation test between field measured carbon and FOTO predicted carbon

		Field observed CarbonCarbon	Foto Predicted carbon
Field observed CarbonCarbon	Pearson Correlation	1	.822**
	Sig. (2-tailed)		.000
	N	20	20
Foto Predicted carbon	Pearson Correlation	.822**	1
	Sig. (2-tailed)	.000	
	N	20	20

**. Correlation is significant at the 0.01 level (2-tailed).

5. DISCUSSION

5.1 Distribution of field measured data

The measurement of DBH has shown significant difference between patch and linear TOF configuration with a p value < 0.05 (refer to table 7 & 8). Hence based on this finding AGB/carbon was separately calculated for linear and patch configuration to avoid biasness and to minimize error propagation. Among the main factors which influenced the difference in DBH measurements between linear and patches TOF configurations can be the difference in management practices. According to Schnell (2015) linear TOF configuration have larger DBH and smaller height when compared to patch TOF configuration. Roadside and windbreaks trees which are considered as linear TOF configuration are constantly subjected to intensive management practices such as spacing, pruning and trimming practices as part of regular inspection of these trees (Johnson, 2000). Whereas trees on forest patches are left for natural regeneration and restoration unless they are looked from production point of view (CGN, 2012).

5.2 Segmentation accuracy

The multi-resolution segmentation accuracy was assessed based on two approaches that is by calculating the "d" value to evaluate the goodness of fit of the segmented and digitized polygons on one hand and by evaluating the 1:1 matching or overlap of segmented and digitized TOF polygons on the other hand (Zhang, 1996). The reference polygons were manually digitized from both linear and patch TOF configuration. Based on these two approaches the overall accuracy of the multi-resolution segmentation process was found to be 72%.

The segmentation accuracy obtained for this study is lower when compared to the segmentation accuracy attained by Mutanga (2012) for delineating TOF in farm lands which achieved an overall accuracy of 72% based on Worldview-2 imagery and Ngwayi (2012) achieved 73% over all accuracy in segmenting TOF using Geo-Eye satellite imagery. On the other hand the segmentation accuracy obtained for this study is higher when compared to the segmentation accuracy attained for a similar study which achieved an overall accuracy of 62% for delineating TOF crowns in urban area (Mustafa et al., 2015). Moreover Geremew (2011) has scored an overall accuracy of 70% which is comparable with the accuracy result obtained in this study for a very similar study area which is located in haagse Bos enschede.

The estimation of precise scale parameter is the first and vital criteria for an accurate delineation of objects of interest in a multi-resolution segmentation process (Dragut et al., 2010). Estimation of scale parameter based on the ESP tool has not yielded a satisfactory result because of the heterogeneity and complexity of the land cover classes involved in the study area in terms of size and spectral responses of objects which have affected the initial segmentation process for the creation of object primitives. Furthermore it was observed from the image that the crown size of trees varies in linear and patch configuration TOF as a result of the difference in canopy structure and specie composition. Hence this in turn has made the selection of precise scale parameter for patch and linear TOF configurations difficult.

Colour which is explained in terms of shape in the homogeneity criterion threshold plays an important role in defining the shape and size of segmented polygons (Blaschke, 2010). However in the Pleiades-1B image used for this study low contrast was observed between different land cover classes resulting on low influence of the colour parameter for accurate delineation of TOF crowns in the multi-resolution

segmentation process. Moreover Lower contrast between background objects and objects of interest which is mainly created by shadow in roadside and windbreak trees makes separability and accurate delineation of tree crowns difficult (Ardila et al., 2007). Filtering or smoothening an image enhances the boundary of tree crowns for better edge detection (Carleer et al., 2005). Hence the 3*3 kernel low pass filtering applied has slightly improved the edge of the tree crowns.

Moreover the similarity in spectral signature that was observed between TOF crowns and some other non-TOF land cover classes has influenced the accurate distinction and delineation of TOF crowns from the other non-TOF land cover classes. In the Pleiades-1B image used for this study TOF and certain grasslands and agricultural fields didn't have distinctive values especially in the red and near infrared band which are the main contributors for successful separation of TOF and non-TOF land cover classes (Hu et al., 2013; Laborte et al., 2010). As it is depicted in figure 27 below the dashed circles indicate the overlap of spectral signature of TOF, grasslands and certain agricultural fields both in the red band and near-infrared band.

To conclude over-segmentation of TOF crowns was slightly higher than under-segmentation of TOF crowns. Moreover according to the visual image inspection done linear TOF configuration are more accurately delineated than patch trees in patch configuration this can be due to less intermingling and crisp crown boundaries in linear TOF configuration (Shimano, 1997). Therefore given the above mentioned points the segmentation accuracy level achieved is adequate to answer research question one of this study.

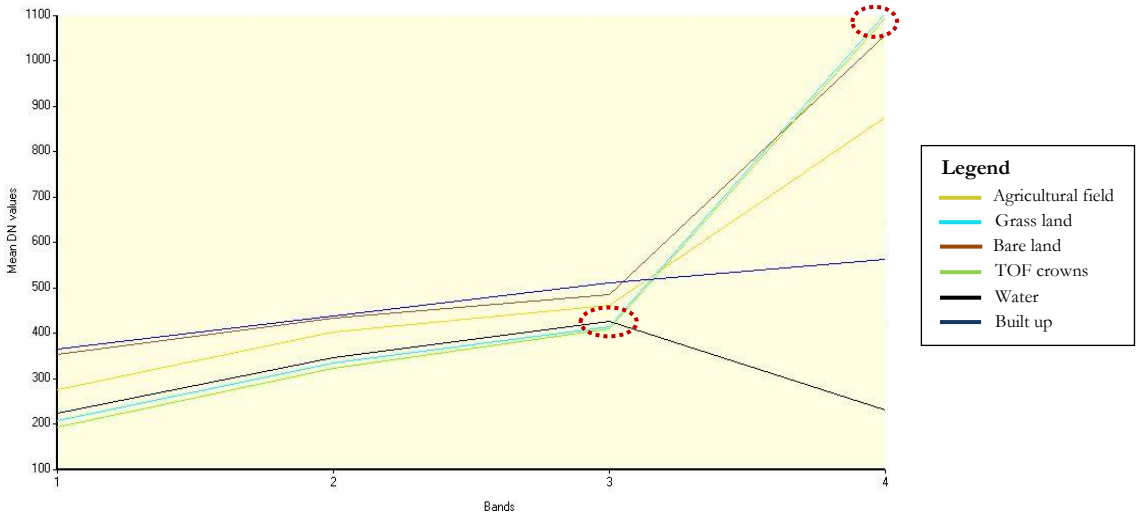

Figure 27. Spectral signature of different land cover classes in the study area

5.3 FOTO method

The Fourier textural ordination (FOTO) method presents a good potential to detect forest canopy structural heterogeneity for Prediction of AGB variations based on aerial photography from GE platform (Ploton et al., 2012). Based on the 2DFFT algorithm in MatLab and PCA analysis of the r-spectra table, the FOTO method generates texture indices which are used as independent variables for AGB and carbon estimation (Barbier et al., 2012). In this study, the first three axes in the PCA analysis explained 73% of the variability observed in the frequency table of r-spectra hence these three principal components were chosen as texture indices for prediction of AGB/carbon of patch TOF configuration. The percentage score of the three texture indices in the PCA analysis is lower in this study when compared to score of the first three axes in other studies were in most cases the first three axes explain more than 80% of the

variation in texture seen in the image (Ploton et al., 2012; Proisy et al., 2007; Singh et al., 2015). The Lower score of the three main axes in the PCA analysis which are chosen as texture indices has in turn influenced the estimation of AGB/carbon based on the FOTO method. The main reasons attributed for the lower score of the texture indices in the PCA analysis can be summarized as:

a) Windowing

Couteron et al. (2005) mentions the selected window size should correspond with the plot size on the ground since the computation of FOTO derived AGB should be correlated based on the plot size. As it is depicted in the figure below the percentage of variation explained by the first three PCA scores increases with the increase in window size(Proisy et al., 2007). However in this study based on the plot size used in the field a window size of 20m*20m was chosen for the 2DFFT analysis which is slightly smaller as compared to the minimum window size used by in other studies (Bastin, 2014; Couteron et al., 2005).

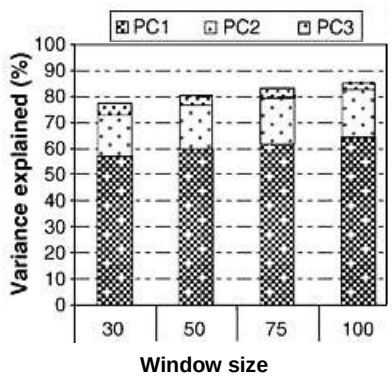

Figure 28. Comparison of different window sizes against PCA scores (Proisy et al., 2007)

b) Masking of non-TOF land cover classes

According to several studies masking out of all land cover classes which are not forest is a perquisite as the presence of objects rather than trees in any given window influences the textural analysis (Meng et al., 2016; Suraj et al., 2016; Ploton et al., 2012). As Proisy et al. (2011) explains the FOTO method is very sensitive to the presence of other land cover classes or gaps rather than trees in any given window because this objects influence the computation of r-spectra resulting in skewed r-spectra value towards low frequencies meaning higher wavelengths which may be mistakenly interpreted as if the canopy contained large tree crowns. However in this study the fuzzy boundary, irregular occurrence pattern and dominance of the non-TOF land cover classes has made complete masking of the other land cover classes such as grass lands and built up areas impossible and very difficult. Hence obtaining a window that constitutes only a continuous tree canopy gradient was difficult as almost all windows in the image include partially or completely other lands cover classes which are not TOF (refer figure 29). Therefore the other land cover classes such as grassland, built up areas and agricultural area were eliminated from the analysis based on their distinctive frequencies after the textural analysis.

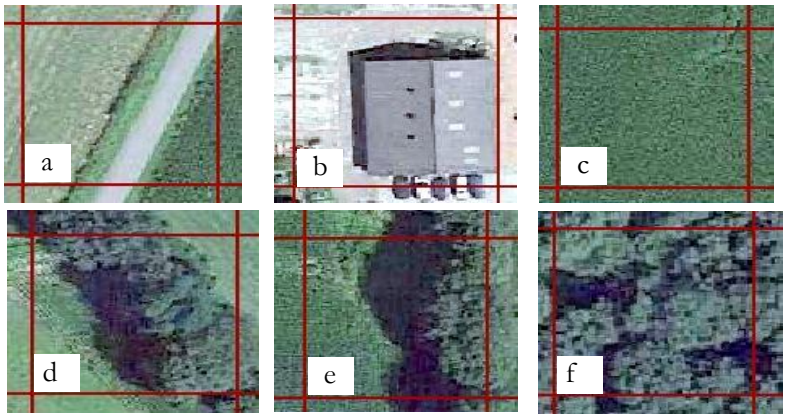

Figure 29. Example of windowing the aerial photography

5.4 AGB/Carbon estimation of TOF

5.4.1 Relationship of remotely sensed CPA and field measured DBH in patch and linear TOF configuration

Several studies (Krajicek et al., 1961; Song et al., 2010; Shah & Acharya, 2010) have proven there is sound relationship between DBH and CPA of trees. However the strength of the relationship between DBH and CPA varies from open-grown trees and trees in patches (Krajicek et al., 1961). Hence for this study the relationship between CPA and DBH in patch TOF configuration was found to be slightly smaller than linear TOF configuration with R^2=0.88 and R^2 =0.78 respectively. However the Pearson correlation coefficients indicate that both relationships are significant at a p value < 0.01. In a patch where there is no gap between trees the individual trees tend to compete more with neighbouring trees for sunlight (Shimano, 1997). Trees start to compete for sunlight when the total crown area of the total number of trees in the patch surpass the patch area (Shimano, 1997).The pipe-model theory explains in closed canopy patches of trees where there is acute shortage of sunlight the lower branches in the canopy start to fall because of shade from surrounding trees however the pipes that used to transport water and food from the fallen branch to the roots will remain in the trunk (Shimano, 1997). That means the pipes which are out of use remain in the tree trunk leading to less strong relationship between DBH and CPA.

On the other hand roadside trees and windbreaks which are grouped in the linear TOF configuration experience less competition with neighbouring trees especially if the tree lines have open canopy structure and in this case the DBH and CPA tend to increase at a similar rate (Krajicek et al., 1961). Even though the spacing between neighbouring trees is small and the crown of two consecutive trees seems to overlap the influence of intermingling is not like in patches. As it is depicted in the figure 30 below the spacing among neighbouring trees during planting and management practices such as trimming in linear TOF configuration leads to less overlap as compared to trees in patches which face crown overlap from all directions.

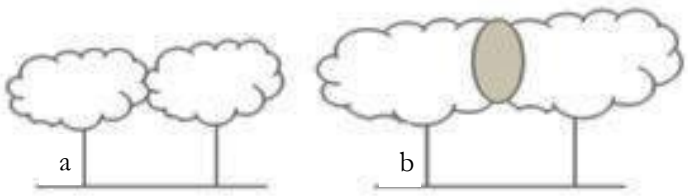

Figure 30. the level of tree intermingling (Shimano, 1997)

In addition to that another important point worth mentioning also might be the crispness of the boundaries of tree crown observed in linear and patch configuration of TOF in very high resolution imagery. According to Shimano (1997) in the forest patches, reflectance of other vegetation, i.e., ground cover, understory shrubs and small trees further creates noise and dominates the reflectance to tree crowns. The boundary of the individual trees that is CPA of trees no longer becomes well defined and crisp. Whereas roadside tree crowns appear well demarcated since most of the trees are usually trimmed and surrounded with man-made geographic objects.

5.4.2 Modelling of carbon from CPA

A non-linear regression model was fitted for the estimation of AGB/carbon of TOF in the study area based on CPA at coefficient of determination 0.89 and 0.82 for linear and patch configuration TOF respectively with 27% RMSE for linear TOF configuration and 34% for patch TOF configuration. The R^2 obtained for both patch and linear TOF configuration is smaller when compared to the R^2 obtained for the estimation of AGB/carbon of both TOF classes for tropical TOF in India which obtained R^2=0.95 and R^2= 0.87 for linear and patch TOF configuration respectively (Pradesh, 2012). However the above studies relied on specie specific local volumetric equations rather than general allometric equations for estimation of biomass/carbon. Where the calculated volume is multiplied with specie specific wood density to obtain AGB/carbon of TOF. Hence the generic allometric equation used in this study as it is discussed in detail in the subsequent section could have influenced the AGB/carbon estimation of TOF. In addition to that the difference in canopy structure and specie composition of trees assessed in different studies could also create difference in model performance. However this study achieved higher result when compared to the result obtained by Geremew (2011) in estimation of AGB/carbon estimation of broad and coniferous trees for the same geographic location.

5.4.3 Modelling of carbon from texture indices

The performance of the FOTO derived carbon was evaluated by plotting the field derived carbon against the FOTO derived carbon for 15 sample plots from the patch configuration. The R^2 value obtained in this research is lower when compared to various studies which were done for AGB/carbon estimation of tropical trees which have a continuous and homogenous tree canopy gradient with less non-tree land over classes based on aerial and GE images (Suraj Reddy et al., 2016; Meng et al., 2016; Ploton et al., 2012). A study for AGB/carbon estimation for a temperate forest in north eastern china has also obtained a satisfactory result with R^2=0.82% using a high resolution IKONOS imagery and R^2=0.76 using a Cartosat-A & F aerial imagery. In this research the relatively smaller window size and presence of non-tree objects in any given window has negatively affected the textural analysis resulting in lower PCA score of the texture indices. This in turn has led to a smaller agreement of the field measured and FOTO measured carbon. As it is mentioned earlier the presence of a continuous tree canopy gradient without obstruction of other non-tree objects is important for the FOTO analysis.

5.4.4 Comparison of FOTO estimated Carbon and OBIA estimated Carbon for patch TOF configuration

The carbon derived from the Pleiades-1B estimation using the OBIA method was compared with the carbon estimated from aerial photography from GE using FOTO method for patch TOF configuration.

The performance of the two methods is estimated based on how the predicted carbon value from the two methods is close to the field measured carbon based on the two estimators of goodness of fit that is R^2 and RMSE value. Coefficient of determination and RMSE value are the two approaches of evaluating the agreement of a predictive model for AGB/carbon with a field measured AGB/carbon which is assumed to give absolute accuracy (Lu, 2006; Muukkonen & Heiskanen, 2005; Meng et al., 2016). The agreement of field measured AGB/carbon and AGB/carbon estimated from remote sensing data with $R^2 \geq 0.7$ is assumed to have strong relationship (Reimann et al., 2011).

The OBIA derived carbon estimation has showed a reasonably good agreement with field measured carbon with R^2 value which is equal to 0.82% and 34% RMSE at a significance level of 0.01. The study has obtained a considerably higher value of R^2 value when compared to the result obtained by Geremew (2011) which has obtained $R^2=0.5$ for both broad leaved and coniferous trees with an 45% RMSE using a linear regression model to predict carbon for a very similar study area in Haagse Bos the Netherlands. However the study has also scored a lower R^2 when compared to the study of Ngwayi (2012) which has obtained $R^2=0.97$ using Geo-Eye imagery for predicting carbon of TOF. As it is discussed earlier the segmentation accuracy, error related with allometric equations and the difference in biophysical characteristics of studies could result in variation of estimation.

The FOTO derived carbon using the three texture indices as predictors of carbon has achieved $R^2=68$ and 39% RMSE when plotted against the field measured carbon per plot from the patch configuration. That is carbon estimation has 68% agreement with field measured biomass at plot level in patch TOF configuration at a significance level of 0.01. The residuals between the FOTO derived carbon and field derived carbon range between -3 ton/plot to +2.7 ton/plot for a plot area of 300 m^2. The R^2 result obtained in this study is generally assumed to be lower when compared to a number of other studies conducted for estimation tree biomass in a homogenous and continuous gradient of trees where the existence of non-tree objects was very negligible unlike this study (Proisy et al., 2011; Singh et al., 2014).

Hence it can be concluded that even though both FOTO and OBIA method has showed significant relationship with field measured carbon, OBIA derived carbon has yielded stronger agreement with field measured carbon both in linear and patch configuration TOF. Whereas FOTO derived carbon has also showed moderate agreement with field measured carbon only for patch configuration TOF. In addition to that, unlike OBIA carbon estimation based on FOTO method was only found to be suitable and convenient for patch configuration TOF which is the inadequacy of FOTO method for a very inclusive TOF assessment that embraces the entire configuration with in it.

5.5 Sources of uncertainity in carbon modelling

Allometric equation

The study has utilized a generic allometric equation suggested by the annex4A.1 guideline of IPCC for temperate hardwood trees since most of the trees surveyed are hardwood trees except for scots pine (IPCC, 2009). The allometric equation uses only tree DBH measurements for estimation of AGB which is suitable since height measurement was assumed to be less accurate especially for patch configuration TOF. There are very few allometric equations which are specifically developed for assessing TOF hence

most studies depend on forest allometric equations that might lead to erroneous estimation of TOF AGB/carbon (Schnell, 2015). Using the same traditional allometric equations as trees inside forest areas for assessing trees outside the forest areas has always been debatable. There are some studies that argue allometric equations for traditional forests misrepresent TOF especially roadside trees and windbreaks (McHale et al., 2009). Low tree density is one important difference linked with TOF as compared to huge forested areas, decreasing the potential competition for light and soil nutrients with neighbouring trees (McHale et al., 2009). Moreover several studies conclude that TOF are often shorter in height and thicker in diameter than trees in forest areas leading to differences in DBH and height with trees in forest environments where most of the allomeric equations represent (Shimano, 1997). In addition to the above mentioned points the management practices applied to traditional forest areas and TOF is also different. TOF are routinely managed for different purposes while on the other hand forests are left for self-restoration and regeneration this also alters the biometric measurement and phenology of trees inside and outside forest area. Based on the above mentioned points the results of the TOF AGB/carbon estimation based on generic allometric equations can be inconclusive and irrespective (McHale et al., 2009; Hunter et al., 2013). Hence the suitability of the available forest allometric equations for TOF AGB/carbon estimation should be tested for an accurate assessment of TOF.

Time difference in image acquisition and field data collection

The time lag between field data collection and the aerial photography from GE is very minimal since the image was taken on 20th of July 2016. Whilst the Pleiades-1B image was acquired on 9th of September 2015 and the field data collection was conducted between from 28th of September to 25th of October. According to Song et al. (2010) the time lag between image acquisition and biometric field data collection lists as an exogenic factor that might affect data quality as a result of growth during the time lag. However planning a field data collection and image acquisition can be very challenging as image acquisition is influenced by a number of circumstances such as weather condition.

Shadow

Image acquisition at a nadir position is not possible with high resolution satellite sensors because nadir position image acquisition negatively influences revisit time of the satellite (Schaaf et al., 1994). However a lot of sensors try to minimize off-nadir sensor position to reduce shadow and other object distortions. In this study the Pleiades-1B image was acquired at 15° off-nadir which has resulted in substantial presence of shadow especially in the linear formation TOF.

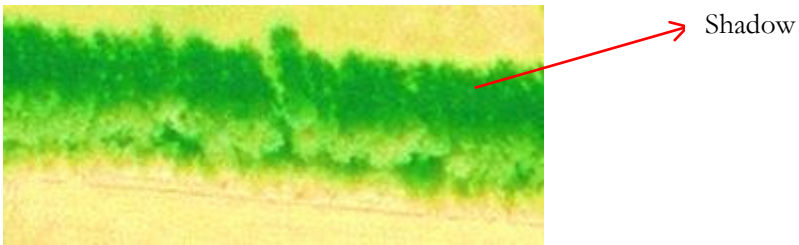

Figure 31. Shadow of trees along a windbreak configuration

Image data in Google earth

The remote sensing data displayed in GE interface has a major limitation in positional accuracy when compared to other very high resolution satellite imageries which ranges from 2 to 46 m for images in Europe (Potere, 2008). However the positional inaccuracy has no influence in the textural analysis since the spatial arrangement of objects doesn't change as a result of the discrepancy in the positional accuracy (Ploton et al., 2012). However it might affect the position of field sample plots used for sampling purposes, however as it is observed from the field this might have small influence on TOF assessments because plots on patch and linear TOF configuration were easily distinguishable both in the GE image and on ground. Moreover GE interface doesn't provide the metadata of images displayed concerning data quality, detailed image acquisition information and the pre-processing techniques especially with regards to aerial photography present with in the GE database that hinders easy tracing of errors and result comprehensiveness (Singh et al., 2015 ; Potere, 2008).

6 CONCLUSION

The study explored the potential of very high resolution satellite imagery and aerial photography from the Google Earth platform to using the OBIA and FOTO method to estimate AGB/carbon of TOF in Gronau Germany. A non- linear regression model was developed using the CPA generated from the segmentation process of the very high resolution Pleiades-1B satellite imagery as an independent variable to estimate the AGB/carbon of both linear and patch TOF configuration based on the OBIA method. Another separate linear multiple regression models was also developed using the texture indices obtained from the FOTO analysis of the aerial photography from Google Earth to predict the AGB/carbon of patch TOF configuration. Hence according to the research objectives and questions of the study the following conclusions are made accordingly:

How accurately can tree crowns in different trees outside the forest (TOF) configurations be segmented?

The segmentation accuracy of the TOF crown of the different configurations was evaluated using a 1:1 matching of the segmented and manually delineated polygons on one hand and by calculating the "D" value which is the measure of goodness of fit on the other hand. Polygons where equally selected from linear and patch TOF configuration for manual delineation, and the overall accuracy was found to be 72%. However according to the visual inspection done it was observed that linear configurations are more accurately segmented than patch TOF configuration.

How significant is the relationship of segmented CPA and field measured DBH of trees between different trees outside the forest (TOF) configurations?

The relationship between CPA segmented from the very high resolution Pleiades-1B image and DBH measured from field for both linear TOF configuration and patch TOF configuration was significant based on the Pearson correlation coefficient analysis done at P level < 0.01. However it was observed that the relationship between CPA and DBH was stronger in linear TOF configuration than the patch TOF configuration with R^2=0.89 for linear TOF configuration and R^2=0.82 for patch TOF configuration.

How significant is the relationship between FOTO predicted above ground biomass (AGB)/carbon and field derived above ground biomass (AGB)/carbon of trees outside the forest (TOF)

The FOTO method was introduced to estimate AGB/carbon of TOF based on the aerial photography form Google Earth. Hence three texture indices obtained from the 2DFFT method in MatLab were chosen as predictor variables for AGB/carbon estimation for patch TOF configuration in the study area. according to the correlation analysis done it was found out that 68% of the FOTO predicted carbon is in agreement with field estimated carbon at R^2=0.68 and RMSE level of 39%. More over the Pearson correlation analysis further supports that the relationship between FOTO predicted and field measured for patch TOF configuration is significant at P level of 0.01.

Which of one of the two remote sensing images used is more accurate for estimation of above ground biomass/carbon of trees outside the forest when compared with field measured above ground biomass/carbon?

The study was conducted to explore the potential of VHR Pleiades-1B imagery and aerial photography from Google Earth using the OBIA and FOTO method to estimate the AGB/carbon of TOF. According to the analysis done both methods are found to be promising. On the endeavours made to discover the merits of aerial photography which is freely available in the Google Earth platform the FOTO method was used to for the purpose of AGB/carbon prediction of TOF in the study area. During the course of the data analysis process it has become clear only patch TOF configuration can suitably be assessed with the FOTO method. Hence the FOTO method was only used to assess the AGB/carbon of TOF. Whereas the OBIA using the very high resolution satellite imagery was found to be suitable for both linear and patch TOF configuration. Hence the AGB/carbon estimation using the FOTO method was compared to the AGB/carbon estimation used for patch configuration only. The models developed for carbon estimation using CPA from OBIA and texture indices from FOTO method were assessed based on the two estimators of goodness of fit that is R^2 and RMSE value. Therefore the model developed based on the CPA generated from OBIA of the very high resolution Pleiades-1B imagery has scored R^2=0.82 and RMSE value of 34%. On the other hand the model developed for prediction of carbon based on the texture indices derived from the FOTO analysis of aerial photography from Google Earth has scored R^2=0.68 and RMSE level of 39%.

LIST OF REFERENCES

Ardila, J. P., Tolpekin, V. A., & Bijker, W. (2007). Context-Sensitive Extraction of Tree Crown Objects in Urban Areas Using Vhr Satellite Images. Retrieved from http://www.boomenbeeld.nl

Barbier, N., Couteron, P., Gastelly-Etchegorry, J. P., & Proisy, C. (2012). Linking canopy images to forest structural parameters: Potential of a modeling framework. *Annals of Forest Science*, *69*(2), 305–311. http://doi.org/10.1007/s13595-011-0116-9

Baró, F., Chaparro, L., Gómez-Baggethun, E., Langemeyer, J., Nowak, D. J., & Terradas, J. (2014). Contribution of ecosystem services to air quality and climate change mitigation policies: the case of urban forests in Barcelona, Spain. *Ambio*, *43*(4), 466–79. http://doi.org/10.1007/s13280-014-0507-x

Bastin, J. (2014). *Estimating the Aboveground Biomass of Central African Tropical Forests at the Tree, Canopy and Region Level*. Retrieved from https://orbi.ulg.ac.be/bitstream/2268/179463/1/merged_document (1).pdf

Beucher, S. (1992). The Watershed Transformation Applied to Image Segmentation. *Proceedings of the 10th Pfefferkorn Conference on Signal and Image Processing in Microscopy and Microanalysis*, 299–314. http://doi.org/10.1.1.24.5229

Blaschke, T. (2010). Object based image analysis for remote sensing. *ISPRS Journal of Photogrammetry and Remote Sensing*, *65*(1), 2–16. http://doi.org/10.1016/j.isprsjprs.2009.06.004

Brown, S. (1997). Estimating biomass and biomass change of tropical forests: a primer. *FAO Forestry Paper*, *134*(August), 55. http://doi.org/ISBN 92-5-103955-0

Burden, D. (2006). 22 Benefits of Urban Street Trees, 1–6. Retrieved from http://northlandnemo.org/images/22BenefitsofUrbanStreetTrees.pdf

Burnett, C., & Blaschke, T. (2003). A multi-scale segmentation/object relationship modelling methodology for landscape analysis. *Ecological Modelling*, *168*(3), 233–249. http://doi.org/10.1016/S0304-3800(03)00139-X

Carleer, A. P., Debeir, O., & Wolff, E. (2005). Assessment of very high spatial resolution satellite image segmentations. *Photogrammetric Engineering and Remote Sensing*, *71*(11), 1285–1294. http://doi.org/10.1117/12.511027

CGN. (2012). First National Report on Forest Genetic Resources for Food and Agriculture, (November), 72. Retrieved from http://documents.plant.wur.nl/cgn/literature/reports/Rapport

CGN-23.pdf

Chave, J., R??jou-M??chain, M., B??rquez, A., Chidumayo, E., Colgan, M. S., Delitti, W. B. C., … Vieilledent, G. (2014). Improved allometric models to estimate the aboveground biomass of tropical trees. *Global Change Biology*, *20*(10), 3177–3190. http://doi.org/10.1111/gcb.12629

Clemens Reimann, Peter Filzmoser, Robert Garrett, R. D. (2011). *Statistical Data Analysis Explained: Applied Environmental Statistics with R - Clemens Reimann, Peter Filzmoser, Robert Garrett, Rudolf Dutter - Google Books*. John Wiley & Sons. Retrieved from https://books.google.nl/books?hl=en&lr=&id=EyjYMb-mTfAC&oi=fnd&pg=PA1979&dq=statistical+data+analysis+explained:+applied+environmental+statstics+with+r&ots=Q-T7MzUBXo&sig=ky71XKMJc8p1Qq_rjhhThuiRhoo#v=onepage&q&f=false

Clinton, N., Holt, A., & Yan, L. (2008). Aa Accuracy Assessment Measure for Object Based Image Segmentation.

Couteron, P., Pelissier, R., Nicolini, E. A., & Paget, D. (2005). Predicting tropical forest stand structure parameters from Fourier transform of very high-resolution remotely sensed canopy images. *Journal of Applied Ecology*, *42*(6), 1121–1128. http://doi.org/10.1111/j.1365-2664.2005.01097.x

Darwish, a., Leukert, K., & Reinhardt, W. (2003). Image segmentation for the purpose of object-based classification. *IGARSS 2003. 2003 IEEE International Geoscience and Remote Sensing Symposium. Proceedings (IEEE Cat. No.03CH37477)*, *3*(C), 2039–2041. http://doi.org/10.1109/IGARSS.2003.1294332

Davies, Z. G., Edmondson, J. L., Heinemeyer, A., Leake, J. R., & Gaston, K. J. (2011). Mapping an urban ecosystem service: quantifying above-ground carbon storage at a city-wide scale. *Journal of Applied Ecology*, *48*(5), 1125–1134. http://doi.org/10.1111/j.1365-2664.2011.02021.x

Definiens. (2007). User guide ecognition. *GIS-Business*, (9), 34–37. Retrieved from http://ecognition.cc/download/userguide.pdf

Definiens. (2009). Definiens Developer 7. Reference Book. Retrieved from http://www.ecognition.cc/download/ReferenceBook.pdf

DeFries, R., Achard, F., Brown, S., Herold, M., Murdiyarso, D., Schlamadinger, B., & de Souza, C. (2007). Earth observations for estimating greenhouse gas emissions from deforestation in developing countries. *Environmental Science & Policy*, *10*(4), 385–394.

http://doi.org/10.1016/j.envsci.2007.01.010

Drăguţ, L., Tiede, D., & Levick, S. R. (2010). ESP: a tool to estimate scale parameter for multiresolution image segmentation of remotely sensed data. *International Journal of Geographical Information Science*, *24*(6), 859–871. http://doi.org/10.1080/13658810903174803

FAO. (2003). Training manual on inventory of trees outside forests (TOF). Retrieved from http://www.fao.org/docrep/006/ac840e/ac840e02.htm

Fridman, J., Holm, S., Nilsson, M., Nilsson, P., Ringvall, A., & Ståhl, G. (2014). Adapting National Forest Inventories to changing requirements – the case of the Swedish National Forest Inventory at the turn of the 20th century. *Silva Fennica*, *48*(3). http://doi.org/10.14214/sf.1095

G. S. Pujar, a, *, P. M, . Reddy, c, … b. (2014). Estimation of Trees Outside Forests using IRS High Resolutio n data by Object Based Image Analysis. *ISPRS*, *XL-8*.

Gibbs, H. K., Brown, S., Niles, J. O., & Foley, J. A. (2007). Monitoring and estimating tropical forest carbon stocks: making REDD a reality. *Environmental Research Letters*, *2*(2007), 45023. http://doi.org/10.1088/1748-9326/2/4/045023

Hay, G. J., & Castilla, G. (2006). Object-based image analysis: strengths, weaknesses, opportunities and threats (SWOT). *International Archives of Photogrammetry Remote Sensing and Spatial Information Sciences*, *36*, 4. http://doi.org/10.1007/978-3-540-77058-9_4

Herrera-Fernández, B. (2003). Classification and modeling of trees outside forest in central American landscapes by combining remotely sensed data and GIS. *Forstwissenschaftliche Fakultät, Doktor*, 222. Retrieved from http://www.ecognition.com/sites/default/files/347_bernal_herrera_doctoral_theses.pdf

Herrera, B., Kleinn, C., Koch, B., & Dees, M. (2004). Automatic Classification of Trees outside Forest using an Object-driven Approach: an Application in a Costa Rican Landscap. *Photogrammetrie, Fernerkundung, Geoinformation 8*, *8*(2), 111–119.

Hu, Q., Wu, W., Xia, T., Yu, Q., Yang, P., Li, Z., & Song, Q. (2013). Exploring the use of google earth imagery and object-based methods in land use/cover mapping. *Remote Sensing*, *5*(11), 6026–6042. http://doi.org/10.3390/rs5116026

Hubert de Foresta, I., Eduardo Somarriba, C., August Temu, I., Boulanger, D., Feuilly, H., & Michelle Gauthier. (2013). T Owards the a Ssessment of.

Hunter, M. O., Keller, M., Victoria, D., & Morton, D. C. (2013). Tree height and tropical forest

biomass estimation. *Biogeosciences*, *10*(12), 8385–8399. http://doi.org/10.5194/bg-10-8385-2013

Hussin, Y. A., Gilani, H., van Leeuwen, L., Murthy, M. S. R., Shah, R., Baral, S., … Qamer, F. M. (2014). Evaluation of object-based image analysis techniques on very high-resolution satellite image for biomass estimation in a watershed of hilly forest of Nepal. *Applied Geomatics*, *6*(1), 59–68. http://doi.org/10.1007/s12518-014-0126-z

IPCC. (2003). Glossary. *Good Practice Guidance for Land Use, Land-Use Change and Forestry*. Retrieved from http://www.ipcc-nggip.iges.or.jp/public/gpglulucf/gpglulucf_files/Glossary_Acronyms_BasicInfo/Glossary.pdf

IPCC. (2007). *Climate Change 2007: Synthesis Report*.

IPCC Annex 4A, Y. (2009). Tools for Estimating Carbon IPCC, *224*, 625–626. Retrieved from http://www.ipcc-nggip.iges.or.jp/public/gpglulucf/gpglulucf_files/Chp4/Chp4_4_Annexes.pdf%5Cnhttp://www.worldagroforestrycentre.org/sea/Publications/files/paper/PP0186-06.PDF

Itoe Constantine Nfor Ngwayi. (2012). *Mapping Carbon Stock in Trees Outside Forest: Comparing a very High Resolution Optical Satellite Image (Geo - Eye) and Airborne LIDAR Data in CHITWAN , NEPAL*. University of Twente.

Jennings, S. B., Brown, N. D., & Sheil, D. (1999). Assessing forest canopies and understorey illumination: canopy closure, canopy cover and other measures. *Forestry*, *72*(1), 59–74. http://doi.org/10.1093/forestry/72.1.59

Johnson, A. (2000). Best Practices Handbook on Roadside Vegetation Management. *Professional Engeneering Services, Ltd.*, 132. Retrieved from http://www.lrrb.org/PDF/200019.pdf

Johnson, K. D., Birdsey, R., Cole, J., Swatantran, A., O'Neil-Dunne, J., Dubayah, R., & Lister, A. (2015). Integrating LIDAR and forest inventories to fill the trees outside forests data gap. *Environmental Monitoring and Assessment*, *187*(10). http://doi.org/10.1007/s10661-015-4839-1

Kajimoto, T., Matsuura, Y., Sofronov, M. A., Volokitina, A. V, Mori, S., Osawa, A., & Abaimov, A. P. (1999). Above- and belowground biomass and primary productivity of a Larix gmelinii stand near Tura, central Siberia. *Tree Physiology*, *19*(12), 815–822. http://doi.org/10.1093/treephys/19.12.815

Kleinn, C. (2000). On large-area inventory and assessment of trees outside forests. *Unasylva*, *51*(200), 3–10.

Krajicek, J., Brinkman, K., & Gingrich, S. (1961). Crown competition-a measure of density. *Forest Science*, *7*(1), 35–42. Retrieved from http://apps.webofknowledge.com/full_record.do?product=UA&search_mode=Refine&qid=2&SID=Q1GFC2af9sNP9Fxe6bR&page=1&doc=2

Laborte, A. G., Maunahan, A. A., & Hijmans, R. J. (2010). Spectral signature generalization and expansion can improve the accuracy of satellite image classification. *PLoS ONE*, *5*(5). http://doi.org/10.1371/journal.pone.0010516

Long, A. J., & Nair, P. K. R. (1999). Trees outside forests: agro-, community, and urban forestry. *New Forests*, *17*(1–3), 145–174. http://doi.org/10.1023/A:1006523425548

Lu, D. (2006). The potential and challenge of remote sensing-based biomass estimation. *International Journal of Remote Sensing*, *27*(7), 1297–1328. http://doi.org/10.1080/01431160500486732

McHale, M. R., Burke, I. C., Lefsky, M. A., Peper, P. J., & McPherson, E. G. (2009). Urban forest biomass estimates: Is it important to use allometric relationships developed specifically for urban trees? *Urban Ecosystems*, *12*(1), 95–113. http://doi.org/10.1007/s11252-009-0081-3

Meneguzzo, D. M., Liknes, G. C., & Nelson, M. D. (2013). Mapping trees outside forests using high-resolution aerial imagery: a comparison of pixel- and object-based classification approaches. *Environmental Monitoring and Assessment*, *185*(8), 6261–6275. http://doi.org/10.1007/s10661-012-3022-1

Meng, S., Pang, Y., Zhang, Z., Jia, W., & Li, Z. (2016). Mapping Aboveground Biomass using Texture Indices from Aerial Photos in a Temperate Forest of Northeastern China. *Remote Sensing*, *8*(3), 230. http://doi.org/10.3390/rs8030230

Möller, M., Lymburner, L., & Volk, M. (2007). The comparison index: A tool for assessing the accuracy of image segmentation. *International Journal of Applied Earth Observation and Geoinformation*, *9*(3), 311–321. http://doi.org/10.1016/j.jag.2006.10.002

Mustafa, Y. T., Habeeb, H. N., Stein, A., & Sulaiman, F. Y. (2015). Identification and Mapping of Tree Species in Urban Areas Using Worldview-2 Imagery. *ISPRS Annals of Photogrammetry, Remote Sensing and Spatial Information Sciences*, *II-2/W2*(October), 175–181. http://doi.org/10.5194/isprsannals-II-2-W2-175-2015

Mutanga, E. (2012). Assessment of Carbon Stocks for Tree Resources on Farmlands Using an Object Based Image Analysis of a Very High Resolution Satellite Image : a Case Study in Ejisu- Juaben District , Ghana Assessment of Carbon Stocks for Tree Resources on Farmlands Using a.

Retrieved from https://www.itc.nl/library/papers_2012/msc/nrm/mutanga.pdf

Muukkonen, P., & Heiskanen, J. (2005). Estimating biomass for boreal forests using ASTER satellite data combined with standwise forest inventory data. *Remote Sensing of Environment*, *99*(4), 434–447. http://doi.org/10.1016/j.rse.2005.09.011

Nowak, D. J., Greenfield, E. J., Hoehn, R. E., & Lapoint, E. (2013). Carbon storage and sequestration by trees in urban and community areas of the United States. *Environmental Pollution*, *178*, 229–236. http://doi.org/10.1016/j.envpol.2013.03.019

Ouyang, Z. (2015). eCognition What is Object-Based Classification. Retrieved from http://lees.geo.msu.edu/courses/geo827/lecture_12a_ecognition.pdf

Ploton, P., Pelissier, R., Proisy, C., Flavenot, T., Barbier, N., Rai, S. N., & Couteron, P. (2012). Assessing aboveground tropical forest biomass using Google Earth canopy images. *Ecological Applications*, *22*(3), 993–1003. http://doi.org/10.1890/11-1606.1

Poorter, H., Niklas, K. J., Reich, P. B., Oleksyn, J., Poot, P., & Mommer, L. (2011). Biomass allocation to leaves, stems and roots: meta-analysis of interspecific variation and environmental control. *New Phytologist*, *193*(1), 30–50. http://doi.org/10.1111/j.1469-8137.2011.03952.x

Potere, D. (2008). Horizontal positional accuracy of google earth's high-resolution imagery archive. *Sensors*, *8*(12), 7973–7981. http://doi.org/10.3390/s8127973

Pradesh, A. (2012). Above-ground standing biomass and carbon stocks of trees outside forests in Prakasam Above-ground standing biomass and carbon stocks of trees outside forests in Prakasam district , (January).

Proisy, C., Barbier, N., Guéroult, M., & Pélissier, R. (2011). Biomass Prediction in Tropical Forests : The Canopy Grain Approach. *Remote Sensing of Biomass: Principles and Applications*, 59–76. http://doi.org/10.5772/696

Proisy, C., Couteron, P., & Fromard, F. (2007). Predicting and mapping mangrove biomass from canopy grain analysis using Fourier-based textural ordination of IKONOS images. *Remote Sensing of Environment*, *109*(3), 379–392. http://doi.org/10.1016/j.rse.2007.01.009

Ryherd, S., & Woodcock, C. (1996). Combining Spectral and Texture Data in the Segmentation of Remotely Sensed Images. *Photogrammetric Engineering Remote Sensing*, *62*(2), 181–194. Retrieved from http://www.asprs.org/publications/pers/96journal/february/1996_feb_181-194.pdf

Schaaf, C. B., Li, X., & Strahler, A. H. (1994). Topographic Effects on Bidirectional and Hemispherical Reflectances Calculated with a Geometric-Optical Canopy Model. *IEEE Transactions on Geoscience and Remote Sensing*, *32*(6), 1186–1193. http://doi.org/10.1109/36.338367

Sebastian Schnell. (2015). Integrating Tre es Outside Forests into National Forest Inventories.

Shah, S. K., & Acharya, H. (2010). Modelling the relationship between canopy projection area and above-ground carbon stock of intermingled canopy trees using high-resolution satellite imagery, 20–29. Retrieved from http://www.nepjol.info/index.php/BANKO/article/viewFile/15463/12498

Shimano, K. (1997). Analysis of the relationship between DBH and crown projection area using a new model. *Journal of Forest Research*, *2*(4), 237–242. http://doi.org/10.1007/BF02348322

Singh, M., Evans, D., Friess, D. A., Tan, B. S., & Nin, C. S. (2015). Mapping above-ground biomass in a tropical forest in Cambodia using canopy textures derived from Google Earth. *Remote Sensing*, *7*(5), 5057–5076. http://doi.org/10.3390/rs70505057

Singh, M., Malhi, Y., & Bhagwat, S. (2014). Biomass estimation of mixed forest landscape using a Fourier transform texture-based approach on very-high-resolution optical satellite imagery. *International Journal of Remote Sensing*, *35*(9), 3331–3349. http://doi.org/10.1080/01431161.2014.903441

Song, C., Dickinson, M. B., Su, L., Zhang, S., & Yaussey, D. (2010). Estimating average tree crown size using spatial information from Ikonos and QuickBird images: Across-sensor and across-site comparisons. *Remote Sensing of Environment*, *114*(5), 1099–1107. http://doi.org/10.1016/j.rse.2009.12.022

Subedi, B., Pandey, S., Pandey, a, & Rana, E. (2010). *Forest Carbon Stock Measurement: Guidelines for measuring carbon stocks in community-managed forests*. *Development*. Retrieved from http://www.forestrynepal.org/publications/book/4772

Suraj Reddy, R., Rajashekar, G., Jha, C. S., Dadhwal, V. K., Pelissier, R., & Couteron, P. (2016). Estimation of Above Ground Biomass Using Texture Metrics Derived from IRS Cartosat-1 Panchromatic Data in Evergreen Forests of Western Ghats, India. *Journal of the Indian Society of Remote Sensing*, (October), 1–9. http://doi.org/10.1007/s12524-016-0630-1

Tenaw Geremew, W. (2011). Assessment of aboveground carbon stock in coniferous and broadleaf forests, using high spatial resolution satellite images, 85. Retrieved from http://www.itc.nl/library/papers_2011/msc/gem/workie.pdf

Wei, W., Chen, X., & Ma, A. (2005). Object-oriented Information Extraction and Application in High-resolution Remote Sensing Image. *Ieee*, *0*(C), 5–8. http://doi.org/10.1109/IGARSS.2005.1525737

Zhan, Q., Molenaar, M., Tempfli, K., & Shi, W. (2005). Quality assessment for geo-spatial objects derived from remotely sensed data. *International Journal of Remote Sensing*, *26*(14), 2953–2974. http://doi.org/10.1080/01431160500057764

Zhang, Y. J. (1996). A survey on evaluation methods for image segmentation. *Pattern Recognition*, *29*(8), 1335–1346. http://doi.org/10.1016/0031-3203(95)00169-7

Zhu, chang qing. (1996). Remote sensing image texture analysis and classification with wavelet transform. Retrieved from http://www.isprs.org/proceedings/XXXI/congress/part3/1036_XXXI-part3.pdf

Zianis, D., & Seura, S. (2005). *Biomass and stem volume equations for tree species in Europe*. *Silva Fennica Monographs* (Vol. 4). Retrieved from http://www.mendeley.com/research/biomass-and-stem-volume-equations-for-tree-species-in-europe/%5Cnhttp://metla.eu/silvafennica/full/smf/smf004.pdf

Zomer, R. J., Trabucco, A., Coe, R., Place, F., Noordwijk, M. Van, & Xu, J. (2014). *Trees on farms : an update and reanalysis of agroforestry ' s global extent and socio-ecological characteristics*.

Appendix 1: Histogram of DBH for different configuration of TOF

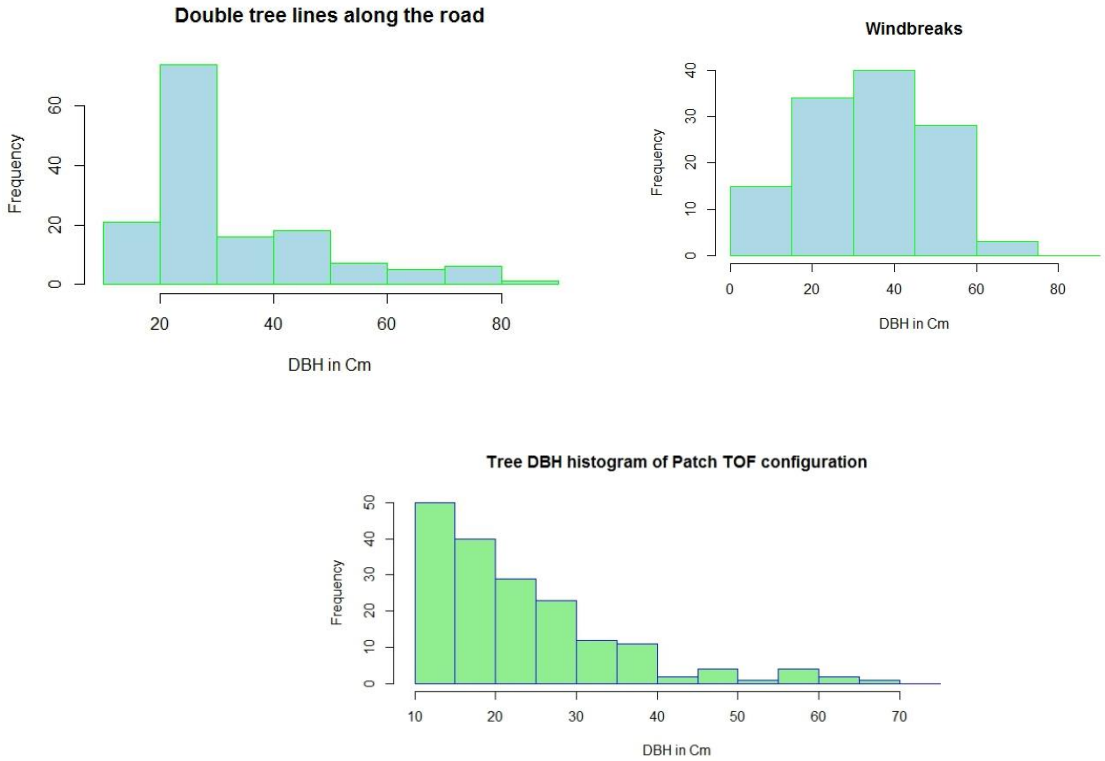

Appendix 2: Histogram of Height for different TOF configurations

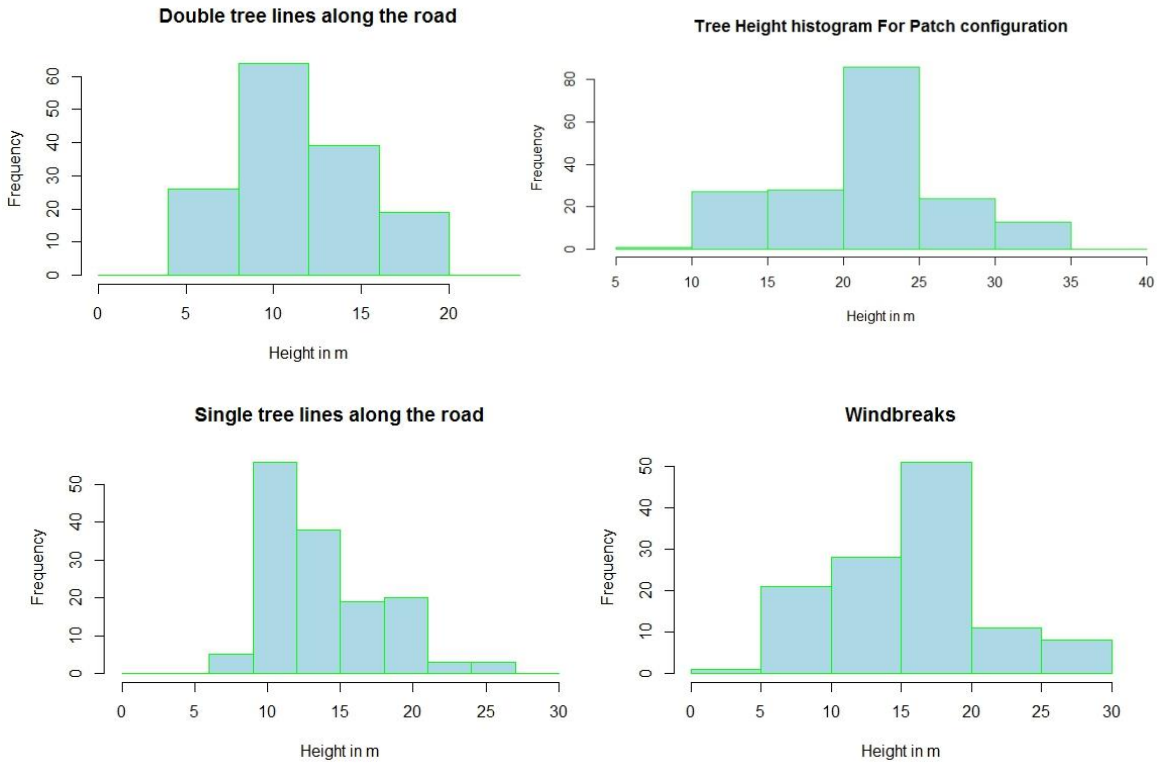

Appendix 3: Collinearity test between CPA and DBH of patch configuration TOF

Correlations

		DBH	CPA
DBH	Pearson Correlation	1	.887**
	Sig. (2-tailed)		.000
	N	94	94
CPA	Pearson Correlation	.887**	1
	Sig. (2-tailed)	.000	
	N	94	94

**. Correlation is significant at the 0.01 level (2-tailed).

Appendix 4: Collinearity test between CPA and DBH of linear configuration TOF

Correlations

		DBH	CPA
DBH	Pearson Correlation	1	.939**
	Sig. (2-tailed)		.000
	N	79	79
CPA	Pearson Correlation	.939**	1
	Sig. (2-tailed)	.000	
	N	79	79

**. Correlation is significant at the 0.01 level (2-tailed).

Appendix 5: Rule set for multi-resolution segmentation of Pleiades-1B satellite imagery

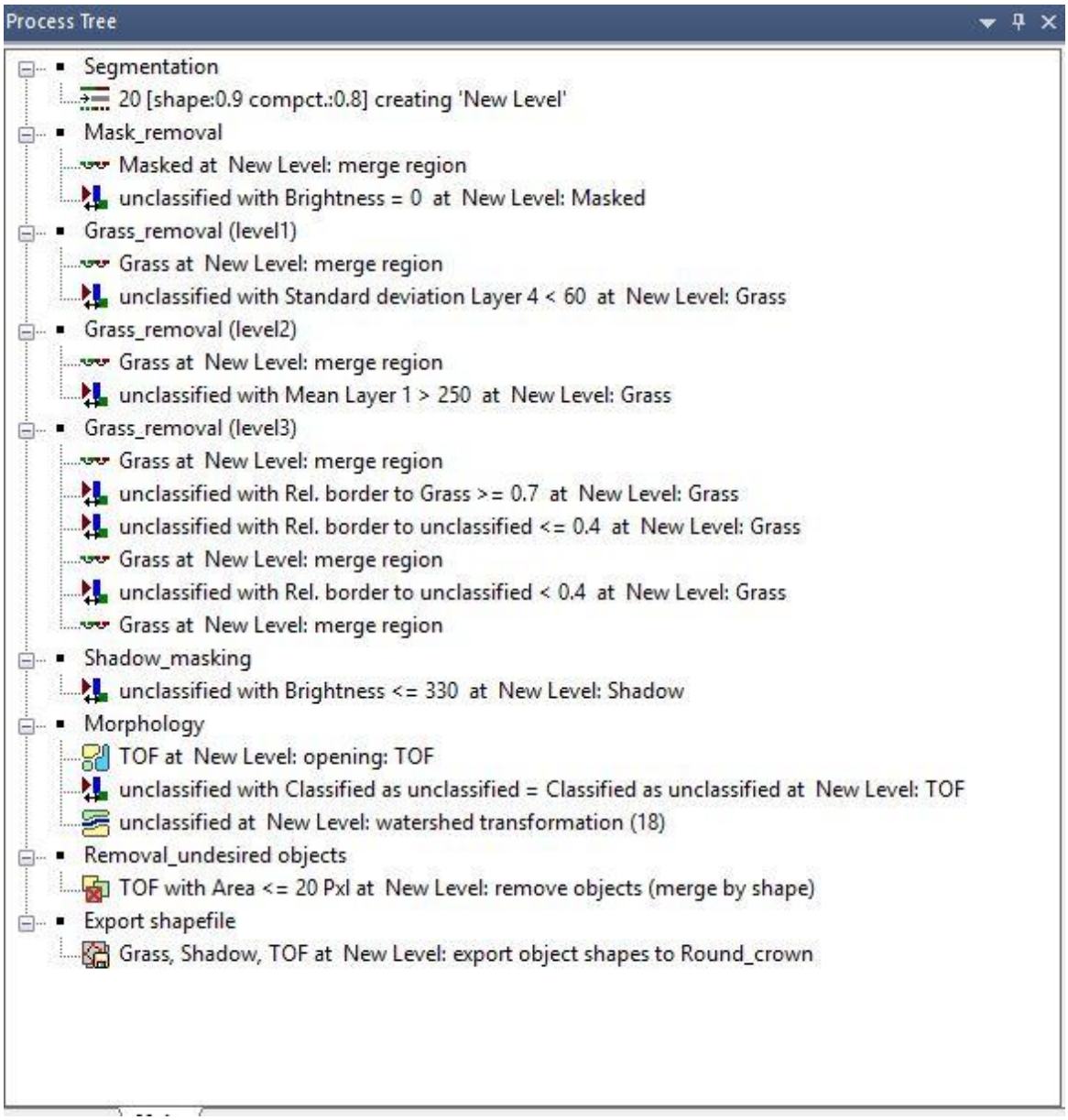

Appendix 6: Field data collection record sheet

	Data Sheet for biomass/carbon estimation in Gronau Germany and Eastern Enschede					**plot No:**
	Date:	**GPS**	X			20
			Y			**Observer Name/Group:**
S. no.	Species (Scientific or/and common name)	DBH (cm)	Height (m)	Configuration class	Remarks	
1	birch	15	24	patch		
2	scots pine	15.6	15			
3	birch	18.7	24			
4	birch	27.8	24			
5	birch	16.3	24			
6	birch	15.2	24			
7	birch	11.2	24			
8	birch	14.5	24			
9	oak	39	28			
10	birch	11	24			
11	oak	18.9	28			
12	birch	12	24			
13	birch	16	24			
14	birch	22	24			
15	birch	20	24			
16	birch	31	24			
17	birch	12	24			
18	birch	13	24			
19	birch	29	24			
20	birch	28	24			
21	birch	24	24			
22	birch	25	24			
23	birch					
24						
25						
26						
27						
28						
29						
30						
31						
	Other Observations:					

Appendix 7: Photos from the field